

Retro-Expert: Collaborative Reasoning for Interpretable Retrosynthesis

Xinyi Li^{1*}, Sai Wang^{1*}, Yutian Lin¹, Yu Wu^{1†}, Yi Yang²

¹School of Computer Science, Wuhan University ²CCAI, Zhejiang University

{xinyil, wangsai23, yutian.lin, wuyucs}@whu.edu.cn

yangyics@zju.edu.cn

Abstract

Retrosynthesis prediction aims to infer the reactant molecule based on a given product molecule, which is a fundamental task in chemical synthesis. However, existing models rely on static pattern-matching paradigm, which limits their ability to perform effective logic decision-making, leading to black-box decision-making. Building on this, we propose Retro-Expert, an interpretable retrosynthesis framework that performs collaborative reasoning by combining the complementary reasoning strengths of Large Language Models and specialized models via reinforcement learning. It outputs natural language explanations grounded in chemical logic through three components: (1) specialized models analyze the product to construct high-quality chemical decision space, (2) LLM-driven critical reasoning to generate predictions and corresponding interpretable reasoning path, and (3) reinforcement learning optimizing interpretable decision policy. Experiments show that Retro-Expert not only surpasses both LLM-based and specialized models across different metrics but also provides expert-aligned explanations that bridge the gap between AI predictions and actionable chemical insights.

1. Introduction

Retrosynthesis prediction aims to deduce potential reactants and reaction pathways for synthesizing a target product molecule based on its structural characteristics [25, 30, 32], holding significant application value in drug discovery and molecular design [14, 35, 38]. However, existing models primarily adopt a pattern-matching paradigm, which learn mappings between product SMILES and reactant SMILES from datasets, framing the task as either classification or auto-regressive sequence generation [4, 34, 46]. Under this paradigm, traditional specialized models capture intricate structural features to learn improved map-

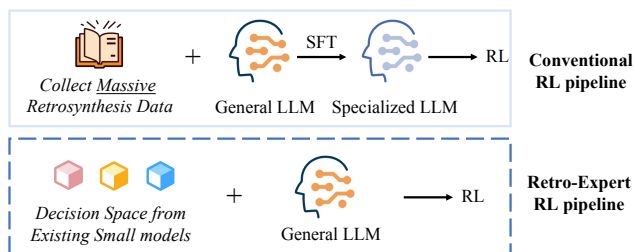


Figure 1. Comparison between the conventional RL pipeline and our methods. Conventional methods require SFT as a necessary step for effective RL, whereas our methods directly optimizes the LLM by leveraging the decision space.

plings, yet their black-box prediction mechanism inherently limits their ability to provide chemically-grounded rationales for their outputs. In contrast, large language models (LLMs) rely on supervised fine-tuning (SFT) to enhance retrosynthetic capabilities, but their performance depends heavily on memorized reaction patterns and typically outputs only reactants or corresponding options [44, 45]. This reliance limits their capacity to understand underlying chemical principles and perform logical reasoning. This paradigm faces three key limitations: (1) The model only generates reactant SMILES strings, with no transparency in its internal reasoning process. (2) The predictions lack natural language explanations grounded in chemical logic, critically hindering real-world adoption. (3) The pure pattern-matching mechanism significantly constrains the model’s capacity for effective logical decision-making. These limitations lead to a lack of reliable basis for the predictions in chemical principles, which severely undermines chemists’ trust in practical applications.

Given the mentioned challenges, a reasoning-driven paradigm aligns more closely with the intrinsic nature of retrosynthetic analysis than simplistic pattern matching. This approach mirrors the strategy employed by chemical experts, who conceptualize retrosynthesis as an iterative and logical reasoning process. Notably, recent breakthroughs in other domains [5, 36, 39] have demonstrated the potential

*These authors contributed equally to this work.

†Corresponding author.

of LLMs to address complex specialized problems through specialized-knowledge-based reasoning, enhanced by reinforcement learning. These findings motivate us to explore how to leverage LLMs’ emergent reasoning capabilities to enhance the interpretability of retrosynthesis prediction.

We focus on chemical knowledge-based retrosynthetic reasoning by LLMs to generate reactants along with an explainable reasoning process, ensuring interpretable and transparent retrosynthesis prediction. To induce reasoning, the selection of an appropriate learning paradigm is crucial. Supervised Fine-Tuning (SFT) inclines models towards replicating prevalent reaction patterns observed in training data, rather than engaging in reasoning grounded in underlying chemical principles. In contrast, Reinforcement Learning (RL) approaches, which optimize the models’ behavioral policy through reward feedback, offer a theoretically viable path to incentivize the complex and logical reasoning abilities for chemical tasks.

However, directly applying RL to incentivize models for retrosynthetic reasoning faces two critical challenges: (1) **Domain Knowledge Disparity.** Retrosynthesis demands not only logical reasoning but also mastery of specialized chemical knowledge. Pre-trained LLMs fail to adequately internalize and apply specific chemical principles when reasoning solely based on molecular SMILES. (2) **Granularity Mismatch in Specialized Capabilities.** The retrosynthetic reasoning process comprises multiple subtasks with distinct cognitive requirements, including reaction type classification and reaction center localization [9, 37, 40]. While general LLMs demonstrate profound logical reasoning abilities, they inherently lack precise perception and matching capabilities for fundamental chemical reaction patterns - a critical requirement for certain subtasks. In contrast, dedicated specialized models, each individually optimized for a specific subtask, have achieved strong performance [4, 30, 38]. To bridge this gap, we propose a novel paradigm that synergistically combines: (1) the knowledge grounding capabilities of specialized models with (2) the deep logical reasoning of LLMs. Specifically, specialized models construct high-quality, multi-dimensional chemical decision spaces, upon which LLMs perform logical reasoning to make the prediction process interpretable.

Building upon these insights, we present **Explainable and Cooperative** retrosynthesis framework, **Retro-Expert**, the first explainable retrosynthesis framework that integrates natural language-based expert reasoning with model-agnostic compatibility (in Figure 1). The framework contains three synergistic core components: (1) **Chemical Decision Space Construction.** Leveraging specialized models (e.g., reaction type classifiers, reaction center localization and reactant generators) to construct high-quality chemical decision space, which provides “knowledge anchors” for LLM’s subsequent deep reasoning. (2) **Collaborative**

Reasoning Engine. Leveraging the effective collaboration with specialized models, the LLM perform integrated critic analysis and in-depth reasoning upon the chemical decision space. It produces the final reactant prediction along with interpretable, natural language-based reasoning process. (3)

Knowledge-Guided Policy Optimization. Retro-Expert optimizes the LLM’s reasoning strategy via rule-based reinforcement learning. A multi-stage reward mechanism is designed during training to guide the model toward learning an optimal and trustworthy reasoning path. Notably, Retro-Expert allows seamless integration of arbitrary specialized models during inference, enabling flexible expansion and adaptation without requiring retraining.

Our contributions are summarized as follows:

1. This work represents the first retrosynthesis model capable of generating natural language interpretable reasoning processes. It fills a long-standing interpretability gap in the field, significantly enhancing chemists’ trust in the model and its practical applicability in real-world scenarios.
2. We propose a collaborative retrosynthesis reasoning framework built upon the synergy between the LLM and specialized models. It improves prediction accuracy while generates human-understandable analysis.
3. Systematic experiments validate the advantages of the LLM-specialized model collaborative reasoning in Retro-Expert. Furthermore, its performance scales with improvements in specialized model accuracy, demonstrating strong generalization and scalability.

2. Related Work

Retrosynthesis Prediction. Existing retrosynthesis methods are broadly categorized into two modeling paradigms: specialized machine learning (ML) models and large language model (LLM)-based methods. ML-based approaches model chemical molecules from different perspectives (e.g., SMILES strings, molecular graphs) to learn the mapping from product to reactant molecules [4, 23, 30, 48]. Although these methods demonstrate significant potential through precise molecular mappings, their black-box decision-making mechanisms inherently restrict the model’s interpretability.

LLM-based approaches aim to enhance the comprehension and memorization capabilities of LLMs for chemical tasks. Some efforts tailor LLMs to retrosynthesis via SFT [42, 44, 45]. Limited by the memorization-centric nature of SFT, these models tend to replicating memorized reaction patterns and only produce predicted reactants or corresponding options. Other work integrates the LLM with external tools to improve prediction accuracy [1, 2, 18]. However, they are limited to directly adopting or scoring based on predefined metrics of specialized model predictions. Such strategies lack engagement in the predictive process and thus fail to provide interpretable reasoning path-

ways that reveal underlying reaction mechanisms.

Large Language Model Reasoning. In recent years, the profound reasoning capabilities of large language models (LLMs) have been developed to solve specialized scientific problems [21, 22, 31, 33]. While employing SFT [15, 49], the model primarily learns to replicate common reasoning patterns from curated datasets, restricting its effectiveness on more complex tasks. In contrast, reinforcement learning (RL)-based reasoning models recently achieve significant progress [8, 11, 50]. In the chemistry field, some studies have assessed the performance of LLMs on chemical reasoning tasks [7, 12]. These models predominantly focus on enhancing performance through SFT paradigm. However, there are few studies that incorporate expert-level reasoning strategies to tackle complex chemical reasoning tasks.

3. Methodology

3.1. Overview

Retro-Expert is to enhance prediction accuracy while generating human-understandable reasoning process. As illustrated in Figure 2, Retro-Expert is built upon three core modules. The process starts with Chemical Decision Space Construction, where specialized models analyze the target product and construct an anchored chemical decision space. This foundation activates the Collaborative Reasoning Engine, where the LLM performs deep reasoning by critically analyzing candidates, selecting an optimal path, and articulating its multi-step logic into a complete natural language chain. Finally, Knowledge-Guided Decision Policy Optimization employs RL to refine the LLM’s decision-making strategy, using a multi-stage reward mechanism to guide it towards an optimal and trustworthy reasoning path.

3.2. Problem Formulation

The objective of the retrosynthesis task T_{retro} is to predict the set of reactants $\{M_r^i\}_{i=1}^C$ ($C \geq 1$) corresponding to a target product M_p . According to chemical expert knowledge, the overall task can be decomposed into s logically connected subtasks $T_{\text{retro}} = \{T_0, T_1, \dots, T_s\}$. Given an environment \mathcal{E} containing S ($S \geq s$) specialized models $\mathcal{M} = \{m_0, m_1, \dots, m_S\}$, each model m_i performs experience-based domain-specific reasoning to generate Top- N candidate predictions P_i for its corresponding subtask:

$$P_i = \{P_i^n\}_{n=1}^N, \quad P_i^n \sim p(m_i | M_p; \theta), \quad (1)$$

where θ denotes the parameters of model m_i , and P_i^n represents the n -th candidate result. The chemical decision space \mathcal{T} is defined as the Cartesian product of candidate results from all subtasks:

$$\mathcal{T} = (P_0, P_1, \dots, P_s), \quad (2)$$

with a space size of K^s . Upon this space, an LLM M_{LLM} interacts with \mathcal{E} , critically analyzes the Top- N candidates from models in \mathcal{M} , and infers the correct answer P'_i for the subtask. This generates a reasoning path $\mathcal{T}_{\text{LLM}} = (P'_0, P'_1, \dots, P'_s)$ alongside a natural-language explanation R . Retro-Expert has two core objectives: generating the correct set of reactants $\hat{a} = \{M_r^i\}_{i=1}^C$, and identifying the optimal path T^* with the highest reward within \mathcal{T} :

$$\begin{aligned} & \arg \max_{\mathcal{T}_{\text{LLM}} \in \mathcal{T}} \text{RM}(\mathcal{T}_{\text{LLM}}) \\ \text{s.t. } & M_{\text{LLM}}(M_p, \mathcal{T}_{\text{LLM}}) = \hat{a}. \end{aligned} \quad (3)$$

Here, $\text{RM}(\cdot)$ is a reward function evaluating the quality of the reasoning path. This framework improves the accuracy of the explainable reasoning R by simultaneously ensuring correct reactant prediction and maximizing the path reward—a critical enhancement not addressed in prior work.

3.3. Chemical Decision Space Construction

Due to the lack of domain-specific knowledge and experience, general LLMs face challenges in retrosynthesis when relying solely on molecular SMILES. Existing methods rely on SFT on large structured chain-of-thought (CoT) data for effective RL. Meanwhile, directly applying RL often fails to efficiently explore feasible reasoning paths under limited sampling, making it difficult for training to progress.

To overcome these challenges, we propose the chemical decision space, which provides LLMs with chemically meaningful starting points for reasoning. This design enables the model to explore feasible reaction pathways more efficiently while maintaining flexibility in its reasoning process. Specifically, for a given target product M_p , we first decompose the retrosynthesis task into a set of distinct chemical sub-tasks such as reaction type prediction and reaction center localization. We then invoke a suite of specialized models optimized for high recall, each dedicated to a sub-task, to generate a corresponding set of plausible candidates. These candidate sets are then integrated, with each subtask’s knowledge (e.g., reaction type, reaction center) forming a multi-dimensional decision space. This space provides well-founded “knowledge anchors” that ground the LLM’s subsequent reasoning, enabling knowledge-aware strategic planning and efficient exploration.

3.4. Collaborative Reasoning Engine

Building upon the chemical decision space, the Collaborative Reasoning Engine acts as the framework’s cognitive hub, bridging specialized models with the LLM. This collaborative process shifts the LLM’s role from a mere predictor or tool-caller to an active reasoning agent that navigates the full retrosynthetic path. This cognitive collaboration guides the LLM to shift from “*directly predicting*

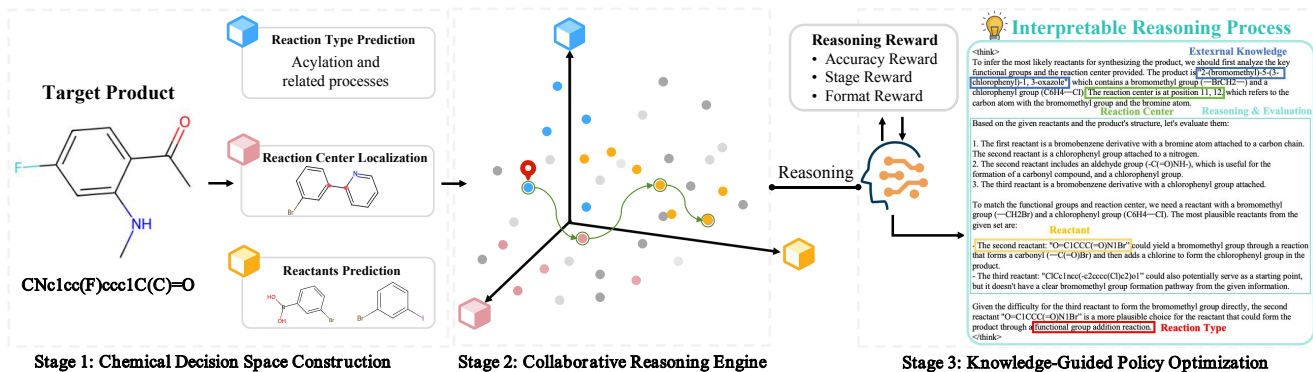


Figure 2. Overview of the Retro-Expert. (1) Decision Space Construction: Specialized models first analyze the target product to construct a high-dimensional chemical decision space composed of high-quality candidate pathways. (2) LLM-driven Navigation: Then, the LLM, acting as a reasoning engine, strategically navigates this space. This involves a critical-generative process where it can either select the best candidate pathway or generate a novel one if all provided options are deemed inadequate. (3) Policy Optimization: Finally, this navigation policy is trained end-to-end via Knowledge-Guided Policy Optimization (KGPO) to ensure the resulting reasoning is both accurate and chemically sound. Please zoom in for a better view of the details.

reactants” to “logical deduction” upon chemical decision space.

The collaborative mechanism is implemented through two key steps: (1) Reasoning Context Construction. Based on the chemical decision space, we combine the candidate sets for each sub-task with external knowledge L to form part of the LLM’s reasoning input. (2) LLM-driven Critical-Generative Reasoning. Within the context, the LLM acts as the active chemical reasoner. In contrast to sequential subtask execution, the LLM autonomously performs logical reasoning by selectively utilizing provided candidate sets, constructing a logically coherent retrosynthetic pathway.

Specifically, the LLM’s autonomous reasoning is a dynamic interplay of two core capabilities: critical analysis and generative decision-making. At each reasoning step, the LLM first rigorously evaluates one candidate set within the provided context. This critical analysis, which ensures a comprehensive exploration of the problem space, directly informs the subsequent decision-making process, which manifests in one of two actions: (1) Selection: The LLM identifies and selects the most plausible candidate from the provided options. (2) Generation: If its analysis concludes that no provided candidate is satisfactory, the LLM leverages its internal knowledge and reasoning context to generate a novel, self-consistent solution. This adaptive reasoning strategy, by mirroring human expert intuition, is therefore not only more efficient and context-aware but also fundamental to enhancing both the accuracy and explainability of the final prediction.

3.5. Knowledge-Guided Policy Optimization

To overcome the limitations of SFT, we introduce a reinforcement learning framework to optimize the LLM’s

reasoning policy within the constructed chemical decision space. The objective function is formally defined as follows:

$$\max_{\pi_{\theta}} \mathbb{E}_{q \sim \mathcal{D}, y \sim \pi_{\theta}(\cdot | q; \mathcal{E})} [r_{\phi}(q, y)] - \beta \mathbb{D}_{kl} [\pi_{\theta}(y | q; \mathcal{E}) \| \pi_{ref}(y | q; \mathcal{E})]. \quad (4)$$

In this objective function, π_{θ} represents the policy model being optimized, while π_{ref} is a reference model used to regularize the policy update, with their divergence measured by \mathbb{D}_{kl} . The term q denotes a query sampled from the dataset, comprising the candidate set \mathcal{T} and any external domain knowledge L . The output y generated by the policy model includes both the complete reasoning path \mathcal{T}_{LLM} and the final predicted reactants a . The optimization aims to maximize the expected reward $r_{\phi}(q, y)$. To optimize this objective, we build upon the Group Relative Policy Optimization (GRPO) algorithm [28]. However, GRPO focus the reward signals solely on the correctness of the final reactant, which limits the model’s performance in chemical reasoning tasks. In practice, a chemist’s trust is earned not by a single, opaque prediction, but by an interpretable reasoning process that aligns with established chemical principles.

To address this limitation, we aim to guide the model toward being “right for the right reasons”, meaning it reaches correct conclusions through chemically valid reasoning. Based on this principle, we propose the Knowledge-Guided Policy Optimization (KGPO) mechanism. The core objective of KGPO is to incentivize the LLM to learn a chemically-grounded reasoning policy that prioritizes the logical validity of the entire pathway, not merely the correctness of the final prediction. It design a novel rule-based, multi-stage reward mechanism tailored to encourage the model to effectively leverage chemical

Table 1. Comparison with LLM-based models on USPTO-50K [24]. Space Setting indicates whether the model is provided with Top-4 reactant candidates and additional domain knowledge anchors (i.e., reaction types, reaction center) from specialized models. General LLMs excel at logical reasoning but lack chemical knowledge. When equipped with a chemical decision space, their performance improves substantially. Results of all LLMs (with/without space) are reported in the Appendix.

Model	Space Setting	Top-1 Acc (%) \uparrow	BLEU \uparrow	Dis \downarrow	Validity \uparrow	MACCS \uparrow	RDKit \uparrow	Morgan \uparrow
<i>LLM-based chemical models</i>								
T5Chem [20]	\times	43.64	0.972	8.42	0.982	0.956	0.974	0.925
ChemFormer [16]	\times	27.30	0.769	14.77	0.952	0.782	0.690	0.647
nach0 [19]	\times	30.52	0.976	11.91	0.990	0.947	0.977	0.905
ChemLLM [44]	\checkmark	12.83	0.869	10.34	0.979	0.851	0.849	0.773
ChemDFM [45]	\times	6.69	0.743	16.62	0.874	0.714	0.807	0.617
ChemCrow (+nach0) [1]	\times	30.52	0.976	11.91	0.990	0.947	0.977	0.905
<i>LLM-based general models</i>								
InterLM-2-Chat-7B	\checkmark	24.31	0.957	11.03	0.895	0.945	0.952	0.909
GPT-3.5	\checkmark	32.93	0.969	7.76	0.991	0.952	0.968	0.913
GPT-4o	\checkmark	32.85	0.970	7.72	0.990	0.953	0.970	0.914
Gemini-2.5-preview-05-20	\checkmark	39.02	0.986	6.63	0.961	0.973	0.989	0.944
Qwen2.5-7B-Instruct [41]	\checkmark	37.55	0.971	7.64	0.992	0.961	0.973	0.922
Ours	\checkmark	70.28	0.998	2.27	0.997	0.990	0.996	0.989

knowledge in the decision space. Specifically, the KGPO framework utilizes a composite reward function that evaluates both the process and outcome. This function is specifically designed to leverage domain knowledge from specialized models, guiding the LLM’s reasoning toward chemical validity while maintaining high accuracy in the final prediction. For a sampled decision path y , it is defined as:

$$r(\mathcal{T}_{\text{LLM}}, y) = \alpha_1 \sum_{i=1}^s r_i + \alpha_2 r_{\text{reactant}} + \alpha_3 r_{\text{format}}, \quad (5)$$

where the term r_i represents the binary stage reward for each of the s sub-tasks. It is assigned a value of 1 if the reasoning process contains correct information for the particular sub-task, and 0 otherwise. r_{reactant} is the reward for the correctness of the final predicted reactants and r_{format} aim to ensure the required output format.

Through KGPO, Retro-Expert fundamentally shifts its focus from “*accuracy-centric prediction*” to the “*generation of coherent and interpretable reasoning chains*”. By optimizing the entire reasoning pathway, the framework produces reasoning that aligns with established principles and expert knowledge, thereby significantly enhancing its practical value and trustworthiness in real-world applications. Furthermore, this process-oriented reward structure inherently mitigates the risk of “reward hacking”, where a model might find a correct answer by a flawed or nonsensical logical path.

4. Experiments

4.1. Experimental Setup

Dataset. We conduct experiments using two benchmark dataset: USPTO-50K [24] and USPTO-FULL [6], which

contain 50k and 1 million atom-mapped reaction records, respectively. We adopt the same training/validation/test splits (8:1:1) as prior works [6]. Following previous methods [30], we canonicalize the product SMILES and reassign the atom-mapping to the corresponding reactant SMILES based on the canonical ordering.

Baselines. We compare Retro-Expert against various strong baselines, categorized into two primary classes: (1) non-LLM-based approaches, including template-based (LocalRetro [4], GLN [6]), semi-template-based (GraphRetro [30], RetroPrime [37], Graph2Edits [47]), and template-free (Retroformer [34], UAlign [43]) models; (2) LLM-based methods, including chemistry-specialized LLMs and general LLMs.

Evaluation Metrics. Inspired by [45], we adopt two complementary sets of metrics to evaluate the performance between the predicted and golden standardized SMILES. The first set focuses on the *textual similarity*, using Top-1 accuracy, BLEU, and levenshtein distance. The second set evaluates the *chemical similarity*, encompassing the validity of the generated SMILES and fingerprint tanimoto similarity (i.e., MACCS, RDKit, Morgan). Additionally, we compare the performance of Retro-Expert against retrosynthesis small models using Top-K accuracy.

Implementation Details. In training, we employ two specialized model for space construction, i.e., T5Chem [20] for reaction type prediction, and GraphRetro [30] for reaction center localization and reactant prediction. During inference, ANY retrosynthetic models can be used to provide reactant candidates in a plug-and-play way, without retraining of the LLM. To balance accuracy and optimization efficiency, we use Top-4 candidate predictions from

Table 2. Comparison with non-LLM-based models on USPTO-50K [24]. Ours indicates the same LLM that reasons over a decision space constructed by the corresponding retrosynthesis model.

Method	Top-K accuracy (%)				Interpretable
	1	3	5	10	
Retroformer [34]	63.5	82.1	86.3	90.2	✗
LocalRetro [4]	63.9	86.8	92.4	96.3	✗
GraphRetro [30]	63.9	81.5	85.2	88.1	✗
GLN [6]	64.2	79.1	85.2	90.0	✗
UAlign [43]	66.2	86.9	91.9	95.1	✗
Graph2Edits [47]	67.2	87.5	91.5	93.8	✗
Ours (Retroformer)	65.5	83.2	86.6	90.1	✓
Ours (LocalRetro)	66.1	88.9	93.1	96.7	✓
Ours (GraphRetro)	66.2	82.4	85.4	88.1	✓
Ours (GLN)	66.5	79.8	85.3	90.0	✓
Ours (UAlign)	69.0	88.9	92.5	95.4	✓
Ours (Graph2Edits)	70.3	89.4	92.1	94.0	✓

each model. We utilize Qwen2.5-7B-Instruct [41] as the LLM and train it using 9k and 80k samples from USPTO-50K [24] and USPTO-FULL [6] datasets, respectively. During training, to prevent reward hacking, we distribute the correct predictions from the specialized model among the Top-4 candidate positions in a 5:3:2 ratio. This strategy prevents the model from developing a positional bias (e.g., always selecting the first candidate) and forces it to learn the intrinsic quality of predictions. The reward weighting coefficients are set as $\alpha_1 = 1.5$, $\alpha_2 = 1.0$, and $\alpha_3 = 0.2$.

4.2. Comparison with State of the Art

Superiority over LLM-based Approaches. As detailed in Table 1, Retro-Expert significantly outperforms both chemistry-focused foundation models and general LLMs, achieving a Top-1 Accuracy improvement of over 26.64%. This demonstrates that our knowledge-guided reinforcement learning approach effectively enhances the model’s reasoning capability. In contrast, the chemical LLMs trained via SFT tend to replicate memorized reaction patterns for prediction. This strategy exhibits suboptimal performance for retrosynthesis prediction.

Superiority over Non-LLM-based Approaches. Beyond outperforming LLMs, Retro-Expert also demonstrates clear advantages over non-LLM-based models (Table 2). When using different retrosynthesis models to construct the reactant-related decision space, Retro-Expert achieves higher Top-K accuracy than the underlying small models. Moreover, our methods exhibits model-agnostic compatibility, enabling seamless integration with various specialized models at no cost (no retraining required). The performance gains scaling proportionally as the baseline model’s own accuracy increases. These results validate that Retro-

Table 3. Comparison of different retrosynthesis methods on the USPTO-FULL [6] dataset.

Method	Top-1 Acc	Top-3 Acc
LocalRetro [4]	39.1	53.3
GLN [6]	39.3	–
Graph2Edits [47]	44.0	60.9
GTA [27]	46.6	–
EditRetro [13]	47.1	61.2
Ours	49.3	63.0

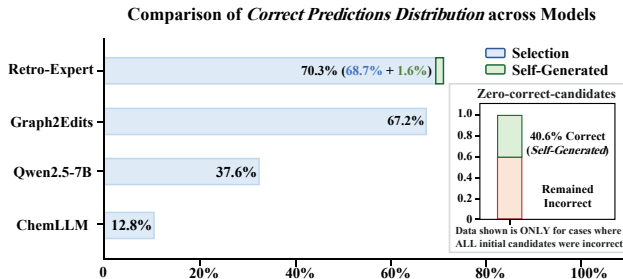


Figure 3. Comparison of correct predictions distributions across different models and Success rate of Retro-Expert’s self-correction mechanism.

Expert effectively reasons over the provided candidate information to optimize its final decision. This collaborative mechanism serves a dual purpose: it boosts the predictive performance of the entire system while making the final choice fully interpretable.

Beyond the USPTO-50K dataset, we further evaluate the performance on the larger and more diverse USPTO-FULL dataset. As shown in Table 3, our method achieves superior performance to existing approaches. This demonstrates that our method is capable of handling more complex and diverse reaction scenarios.

Emergent Capability for Self-reflection. A particularly compelling finding is the emergent capability of Retro-Expert for self-reflection and reasoning, which allows the LLM to overcome the limitations of the input specialized models. The framework does not uncritically accept the candidates provided by specialized models. Instead, it exhibits a capacity for critical analysis and self-correction. As illustrated in Figure 10, when a specialized model fails to provide valid reactant candidates (e.g., they are entirely incorrect or no candidate), Retro-Expert may generate a new correct answer. A statistical analysis of such cases reveals that this self-reflection mechanism achieved a remarkable 40.6% success rate, showing that it is not a selection model but a generative model that can create new answers.

Superior Generalization on Out-of-Distribution Data. We evaluate Retro-Expert’s generalization on the out-of-distribution (OOD) ChemBench benchmark [44], where

Table 4. Top-1 accuracy (%) of different models on the out-of-distribution ChemBench benchmark [44].

Method	Top-1 Accuracy (%)
ChemLLM [44]	15.33
Qwen2.5-7B-Instruct [41]	29.33
DeepSeek-R1 [11]	32.54
Ours	57.00

Table 5. Evaluation on reasoning process using GPT-4o and human expert assessment. MA: Mechanism Accuracy, FC: Factual Correctness, LC: Logic Consistency.

Evaluator	Model	Metrics		
		MA	FC	LC
GPT-4o	Qwen2.5-7B-Instruct	3.67	3.12	4.06
	Ours	4.21	3.89	4.17
Human	Qwen2.5-7B-Instruct	3.21	2.89	3.87
	Ours	4.17	3.69	4.23

94.66% of the 300 reaction pathways are absent from USPTO-50K, reflecting real-world discovery conditions. To ensure fairness, all models shared an identical decision space formulated as a four-option choice task (one ground truth and three distractors). As shown in Table 4, general LLMs achieve accuracy around 30%. In contrast, Retro-Expert attains 57.00% accuracy. This improved generalization is enabled by KGPO, which ingrains a transferable, chemistry-principled reasoning policy.

4.3. Interpretability Evaluation

Since explanatory capabilities are largely absent in specialized chemical models, we benchmarked Retro-Expert against general LLMs on the USPTO-50K test set. These baseline models were explicitly prompted to generate a step-by-step rationale. The evaluation combines GPT-4o automatic scoring with expert human assessment. For the human evaluation, we recruited three independent evaluators, each with experience in synthetic organic chemistry.

We design three core metrics: (1) Mechanism Accuracy (MA): The alignment of the described reaction mechanism with established chemical principles; (2) Factual Correctness (FC): The degree of factual errors in chemical knowledge within the reasoning process; and (3) Logical Consistency (LC): The logic coherence and soundness of the reasoning process. All evaluation metrics was scored on a 1 to 5 point scale, with 5 being the best. Each metric includes a corresponding definition with detailed evaluation criteria. (See Appendix for detailed criteria).

Retro-Expert Delivers Credible Reasoning Superior to General LLMs. As detailed in Table 5, Retro-Expert achieves scores near or above 4.0 in the automated GPT-4o assessment, significantly outperforming the general LLM baselines. This strong performance was largely corroborated by human experts, who awarded high scores for Mechanism Accuracy (MA) and Logical Consistency (LC), confirming that Retro-Expert generates clear, coherent, and mechanistically plausible reasoning pathways. These demonstrated capabilities are crucial for enhancing the transparency and interpretability of the prediction process, fostering greater trust in its real-world application.

Table 6. Performance comparison under different decision space.

Decision Space			Reactants
Type	Center	Reactant	Top-1 Accuracy (%)
		✓	29.1
✓		✓	32.6
	✓	✓	56.7
✓	✓	✓	70.3

Table 7. Performance comparison using different training policy. Top-1 accuracy quantifies reasoning correctness, and MA, FC, and LC assess the reasoning process.

Setting	Reasoning Result	Reasoning Process		
	Top-1 Acc (%)	MA	FC	LC
SFT	48.6	2.75	2.12	2.84
RL (GRPO [28])	66.8	3.37	3.65	3.49
RL (KGPO)	70.3	4.33	3.97	4.25

ated by human experts, who awarded high scores for Mechanism Accuracy (MA) and Logical Consistency (LC), confirming that Retro-Expert generates clear, coherent, and mechanistically plausible reasoning pathways. These demonstrated capabilities are crucial for enhancing the transparency and interpretability of the prediction process, fostering greater trust in its real-world application.

4.4. Ablation Study

We conducted a series of ablation studies to validate the core architectural choices of Retro-Expert. Additional studies are provided in the appendix.

Effective Reasoning Hinges on the Chemical Decision Space. To demonstrate the necessity and effectiveness of constructing chemical decision space, we train LLMs using KGPO under different decision space. As shown in Table 6, when only four candidate reactants are provided, the model’s prediction accuracy is extremely low (29.1%). When gradually add “type”, “center” into the decision space, the performance gradually increases to 70.3%. This indicates that a structured, multi-dimensional decision space is essential to properly ground the LLM’s logical reasoning and achieve high accuracy.

Effectiveness of KGPO for Superior Reasoning. To understand the effectiveness of KGPO in enhancing LLM reasoning, we train LLMs using different training strategies. As shown in Table 7, the KGPO-trained LLM achieves superior performance compared to other baselines. SFT encourages pattern memorization for prediction. This limits the model’s ability to flexibly perform logical reasoning, thereby creating performance bottlenecks in reasoning-intensive tasks such as retrosynthesis. While GRPO improves accuracy, it solely focuses on the final answer’s correctness. This may

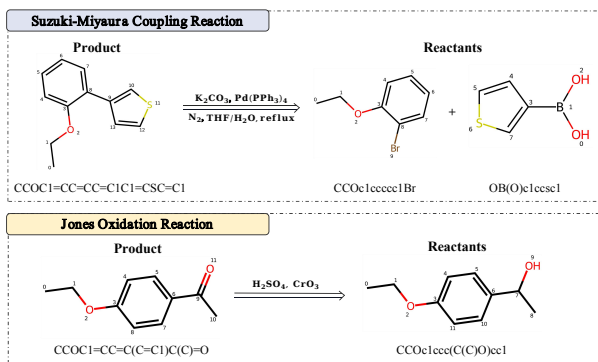


Figure 4. Visualization of the novel reaction pathways proposed by Retro-Expert and validated through wet-lab experiments. The details are provided in the appendix.

lead the model to exploit logically flawed or chemically implausible shortcuts to arrive at the correct conclusion, resulting in suboptimal reasoning outcomes and paths. In contrast, our KGPO strategy effectively guides the model in utilizing the structured decision space, resulting in more accurate prediction. Furthermore, the strategy notably enhances the quality of the reasoning process, improving both the coherence and accuracy of the generated content.

4.5. Wet Lab Experiments

To validate Retro-Expert’s practical utility, we extended beyond in-silico (dry-lab) tests to chemical web-lab experiments, demonstrating its capacity as a genuine engine for chemical discovery. We provide direct experimental evidence that Retro-Expert can successfully propose a feasible synthesis of a molecule that previously lacked any documented production path, and discovers a novel reaction route for an existing compound.

Our experiments successfully validate these two distinct types of chemical discovery. (1) Our Retro-Expert model predicted a new route of **Suzuki-Miyaura coupling** to synthesize 3-(2-ethoxyphenyl)thiophene (CCOC1=CC=CC=C1C1=CSC=C1) via a reaction between 1-bromo-2-ethoxybenzene (CCOc1cccc1Br) and thiophen-3-ylboronic acid (OB(O)c1ccsc1). Crucially, verification using the CAS SciFinder database confirmed that while the compound’s structure was known, no synthesis pathway had ever been published for it. Our work thus constitutes its first-ever reported synthesis, which we successfully achieved with a percent yield of 79.3%. (2) For the well-established molecule 1-(4-ethoxyphenyl)ethanone (CCOC1=CC=C(C=C1)C(C)=O), our model identified a novel **Jones Oxidation** pathway. The target compound can be synthesized via 1-(4-ethoxyphenyl)ethanol (CCOc1ccc(C(C)O)cc1) using chromium trioxide in acidic conditions. This route, confirmed to be an undocumented alternative to existing methods, was also successfully

Table 8. Comparison of different methods on multi-step retrosynthesis (the test set of PaRoutes [10] dataset).

Method	Top-1 Acc (%)
DFPN [17]	11
Retro* [3]	15
MCTS [26]	17
DMS-Deep [29]	36
Ours	38

executed in our chemical lab with a yield of 58.82%. These outcomes offer compelling proof that Retro-Expert is an effective tool for practical chemical discovery.

4.6. Case Study: Making Reasoning Transparent

As visualized on the right side of Figure 2, Retro-Expert generates a human-readable rationale that articulates its critical analysis for a specific molecule. The process begins with the construction of the decision space. For this example, specialized models identify “functional group addition” as a probable reaction type and pinpoint positions 11 and 12 as potential reaction centers. The model’s rationale then demonstrates its navigation of this space. For instance, it correctly discards a candidate reactant, explicitly stating that it is ruled out due to the “absence of a clear bromomethyl group”. The logical and verifiable narrative is essential for enhancing a chemical expert’s trust and boosting the model’s practical applicability.

4.7. Multi-Step Retrosynthesis Prediction

We extend Retro-Expert to enable multi-step retrosynthetic prediction based on the PaRoutes dataset [10]. Specifically, we employ the DMS-Deep [29] model to generate candidates that form the decision space. As shown in Table 8, we report the Top-1 accuracy of different models on the test set. Our proposed method achieves the highest prediction accuracy while generating a natural language-based reasoning process. These results underscore the potential of our model for practical retrosynthesis predictions.

5. Conclusion

We introduced Retro-Expert, a novel retrosynthesis framework to address long-standing interpretability limitations by generating human-readable reasoning process. Our approach synergizes specialized models, which construct a chemical decision space, with an LLM that navigates it using KGPO policy trained via RL. Experiments show Retro-Expert achieves competitive accuracy and strong generalization while allowing for plug-and-play modularity. By bridging the gap between AI prediction and a chemist’s workflow, Retro-Expert represents a significant step toward trustworthy and collaborative AI in chemical discovery.

References

- [1] Andres M Bran, Sam Cox, Oliver Schilter, Carlo Baldassari, Andrew D White, and Philippe Schwaller. Chemcrow: Augmenting large-language models with chemistry tools. *arXiv preprint arXiv:2304.05376*, 2023. 2, 5
- [2] Andres M Bran, Theo A Neukomm, Daniel P Armstrong, Zlatko Jončev, and Philippe Schwaller. Chemical reasoning in llms unlocks steerable synthesis planning and reaction mechanism elucidation. *arXiv preprint arXiv:2503.08537*, 2025. 2
- [3] Binghong Chen, Chengtao Li, Hanjun Dai, and Le Song. Retro*: learning retrosynthetic planning with neural guided a* search. In *International conference on machine learning*, pages 1608–1616. PMLR, 2020. 8
- [4] Shuan Chen and Yousung Jung. Deep retrosynthetic reaction prediction using local reactivity and global attention. *JACS Au*, 1(10):1612–1620, 2021. 1, 2, 5, 6
- [5] Yongrui Chen, Junhao He, Linbo Fu, Shenyu Zhang, Rihui Jin, Xinbang Dai, Jiaqi Li, Dehai Min, Nan Hu, Yuxin Zhang, et al. Pandora: A code-driven large language model agent for unified reasoning across diverse structured knowledge. *arXiv preprint arXiv:2504.12734*, 2025. 1
- [6] Hanjun Dai, Chengtao Li, Connor Coley, Bo Dai, and Le Song. Retrosynthesis prediction with conditional graph logic network. *Advances in Neural Information Processing Systems*, 32, 2019. 5, 6
- [7] Kehua Feng, Keyan Ding, Weijie Wang, Xiang Zhuang, Zeyuan Wang, Ming Qin, Yu Zhao, Jianhua Yao, Qiang Zhang, and Huajun Chen. Sciknowledgeal: Evaluating multi-level scientific knowledge of large language models. *arXiv preprint arXiv:2406.09098*, 2024. 3
- [8] Kaituo Feng, Kaixiong Gong, Bohao Li, Zonghao Guo, Yibing Wang, Tianshuo Peng, Benyou Wang, and Xiangyu Yue. Video-rl: Reinforcing video reasoning in mllms. *arXiv preprint arXiv:2503.21776*, 2025. 3
- [9] Zhangyang Gao, Cheng Tan, Lirong Wu, and Stan Z Li. Semiretro: Semi-template framework boosts deep retrosynthesis prediction. *arXiv preprint arXiv:2202.08205*, 2022. 2
- [10] Samuel Genheden and Esben Bjerrum. Paroutes: towards a framework for benchmarking retrosynthesis route predictions. *Digital Discovery*, 1(4):527–539, 2022. 8
- [11] Daya Guo, Dejian Yang, Haowei Zhang, Junxiao Song, Ruoyu Zhang, Runxin Xu, Qihao Zhu, Shirong Ma, Peiyi Wang, Xiao Bi, et al. Deepseek-rl: Incentivizing reasoning capability in llms via reinforcement learning. *arXiv preprint arXiv:2501.12948*, 2025. 3, 7
- [12] Taicheng Guo, Bozhao Nan, Zhenwen Liang, Zhichun Guo, Nitesh Chawla, Olaf Wiest, Xiangliang Zhang, et al. What can large language models do in chemistry? a comprehensive benchmark on eight tasks. *Advances in Neural Information Processing Systems*, 36:59662–59688, 2023. 3
- [13] Yuqiang Han, Xiaoyang Xu, Chang-Yu Hsieh, Keyan Ding, Hongxia Xu, Renjun Xu, Tingjun Hou, Qiang Zhang, and Huajun Chen. Retrosynthesis prediction with an iterative string editing model. *Nature Communications*, 15(1):6404, 2024. 6
- [14] Zhaolin Hu, Yixiao Zhou, Zhongan Wang, Xin Li, Weimin Yang, Hehe Fan, and Yi Yang. Osda agent: Leveraging large language models for de novo design of organic structure directing agents. In *The Thirteenth International Conference on Learning Representations*, 2025. 1
- [15] Zhongzhen Huang, Gui Geng, Shengyi Hua, Zhen Huang, Haoyang Zou, Shaoting Zhang, Pengfei Liu, and Xiaofan Zhang. O1 replication journey—part 3: Inference-time scaling for medical reasoning. *arXiv preprint arXiv:2501.06458*, 2025. 3
- [16] Ross Irwin, Spyridon Dimitriadis, Jiazhen He, and Esben Jannik Bjerrum. Chemformer: a pre-trained transformer for computational chemistry. *Machine Learning: Science and Technology*, 3(1):015022, 2022. 5
- [17] Akihiro Kishimoto, Beat Buesser, Bei Chen, and Adi Botea. Depth-first proof-number search with heuristic edge cost and application to chemical synthesis planning. *Advances in Neural Information Processing Systems*, 32, 2019. 8
- [18] Zhiyuan Liu, Yaorui Shi, An Zhang, Sihang Li, Enzhi Zhang, Xiang Wang, Kenji Kawaguchi, and Tat-Seng Chua. Reactxt: Understanding molecular “reaction-ship” via reaction-contextualized molecule-text pretraining. *arXiv preprint arXiv:2405.14225*, 2024. 2
- [19] Micha Livne, Zulfat Miftahudinov, Elena Tutubalina, Maksim Kuznetsov, Daniil Polykovskiy, Annika Brundyn, Aastha Jhunjhunwala, Anthony Costa, Alex Aliper, Alán Aspuru-Guzik, et al. nach0: multimodal natural and chemical languages foundation model. *Chemical Science*, 15(22): 8380–8389, 2024. 5
- [20] Jieyu Lu and Yingkai Zhang. Unified deep learning model for multitask reaction predictions with explanation. *Journal of chemical information and modeling*, 62(6):1376–1387, 2022. 5
- [21] Jiazhen Pan, Che Liu, Junde Wu, Fenglin Liu, Jiayuan Zhu, Hongwei Bran Li, Chen Chen, Cheng Ouyang, and Daniel Rueckert. Medvlm-rl: Incentivizing medical reasoning capability of vision-language models (vlms) via reinforcement learning. *arXiv preprint arXiv:2502.19634*, 2025. 3
- [22] Rafa Anugrah Putri, Ahmad Taufiq, et al. Effectiveness of innovative learning models to improve scientific reasoning on physics topics: A literature review. *Jurnal Penelitian Pendidikan IPA*, 11(3):19–22, 2025. 3
- [23] Mikołaj Sacha, Mikołaj Błaz, Piotr Byrski, Paweł Dabrowski-Tumanski, Mikołaj Chrominski, Rafał Loska, Paweł Włodarczyk-Pruszyński, and Stanisław Jastrzebski. Molecule edit graph attention network: modeling chemical reactions as sequences of graph edits. *Journal of Chemical Information and Modeling*, 61(7):3273–3284, 2021. 2
- [24] Nadine Schneider, Nikolaus Stiefl, and Gregory A Landrum. What’s what: The (nearly) definitive guide to reaction role assignment. *Journal of chemical information and modeling*, 56(12):2336–2346, 2016. 5, 6
- [25] Marwin HS Segler and Mark P Waller. Neural-symbolic machine learning for retrosynthesis and reaction prediction. *Chemistry—A European Journal*, 23(25):5966–5971, 2017. 1
- [26] Marwin HS Segler, Mike Preuss, and Mark P Waller. Planning chemical syntheses with deep neural networks and symbolic ai. *Nature*, 555(7698):604–610, 2018. 8

- [27] Seung-Woo Seo, You Young Song, June Yong Yang, Seohui Bae, Hankook Lee, Jinwoo Shin, Sung Ju Hwang, and Eunho Yang. Gta: Graph truncated attention for retrosynthesis. In *Proceedings of the AAAI Conference on Artificial Intelligence*, pages 531–539, 2021. 6
- [28] Zhihong Shao, Peiyi Wang, Qihao Zhu, Runxin Xu, Junxiao Song, Xiao Bi, Haowei Zhang, Mingchuan Zhang, YK Li, Y Wu, et al. Deepseekmath: Pushing the limits of mathematical reasoning in open language models. *arXiv preprint arXiv:2402.03300*, 2024. 4, 7
- [29] Yu Shee, Anton Morgunov, Haote Li, and Victor S Batista. Directmultistep: Direct route generation for multistep retrosynthesis. *Journal of Chemical Information and Modeling*, 65(8):3903–3914, 2025. 8
- [30] Vignesh Ram Somnath, Charlotte Bunne, Connor Coley, Andreas Krause, and Regina Barzilay. Learning graph models for retrosynthesis prediction. *Advances in Neural Information Processing Systems*, 34:9405–9415, 2021. 1, 2, 5, 6
- [31] Yanzhou Su, Tianbin Li, Jiyao Liu, Chenglong Ma, Junzhi Ning, Cheng Tang, Sibojin, Jin Ye, Pengcheng Chen, Ming Hu, et al. Gmai-vl-r1: Harnessing reinforcement learning for multimodal medical reasoning. *arXiv preprint arXiv:2504.01886*, 2025. 3
- [32] Ruoxi Sun, Hanjun Dai, Li Li, Steven Kearnes, and Bo Dai. Towards understanding retrosynthesis by energy-based models. *Advances in Neural Information Processing Systems*, 34:10186–10194, 2021. 1
- [33] Xiangru Tang, Tianyu Hu, Muiyang Ye, Yanjun Shao, Xunjian Yin, Siru Ouyang, Wangchunshu Zhou, Pan Lu, Zhusheng Zhang, Yilun Zhao, et al. Chemagent: Self-updating library in large language models improves chemical reasoning. *arXiv preprint arXiv:2501.06590*, 2025. 3
- [34] Yue Wan, Chang-Yu Hsieh, Ben Liao, and Shengyu Zhang. Retroformer: Pushing the limits of end-to-end retrosynthesis transformer. In *International Conference on Machine Learning*, pages 22475–22490. PMLR, 2022. 1, 5, 6
- [35] Jingxue Wang, Huali Cao, John ZH Zhang, and Yifei Qi. Computational protein design with deep learning neural networks. *Scientific reports*, 8(1):1–9, 2018. 1
- [36] Junxiong Wang, Wen-Ding Li, Daniele Paliotta, Daniel Ritter, Alexander M Rush, and Tri Dao. M1: Towards scalable test-time compute with mamba reasoning models. *arXiv preprint arXiv:2504.10449*, 2025. 1
- [37] Xiaorui Wang, Yuquan Li, Jiezhong Qiu, Guangyong Chen, Huanxiang Liu, Benben Liao, Chang-Yu Hsieh, and Xiaojun Yao. Retroprime: A diverse, plausible and transformer-based method for single-step retrosynthesis predictions. *Chemical Engineering Journal*, 420:129845, 2021. 2, 5
- [38] Yiming Wang, Yuxuan Song, Minkai Xu, Rui Wang, Hao Zhou, and Weiyang Ma. Retrodiff: Retrosynthesis as multi-stage distribution interpolation. *arXiv preprint arXiv:2311.14077*, 2023. 1, 2
- [39] Tian Xie, Zitian Gao, Qingnan Ren, Haoming Luo, Yuqian Hong, Bryan Dai, Joey Zhou, Kai Qiu, Zhirong Wu, and Chong Luo. Logic-rl: Unleashing llm reasoning with rule-based reinforcement learning. *arXiv preprint arXiv:2502.14768*, 2025. 1
- [40] Chaochao Yan, Qianggang Ding, Peilin Zhao, Shuangjia Zheng, Jinyu Yang, Yang Yu, and Junzhou Huang. Retroxpert: Decompose retrosynthesis prediction like a chemist. *Advances in Neural Information Processing Systems*, 33:11248–11258, 2020. 2
- [41] An Yang, Bowen Yu, Chengyuan Li, Dayiheng Liu, Fei Huang, Haoyan Huang, Jiandong Jiang, Jianhong Tu, Jianwei Zhang, Jingren Zhou, et al. Qwen2. 5-1m technical report. *arXiv preprint arXiv:2501.15383*, 2025. 5, 6, 7
- [42] Yifei Yang, Runhan Shi, Zuchao Li, Shu Jiang, Yang Yang, Bao-Liang Lu, and Hai Zhao. Batgpt-chem: a foundation large model for chemical engineering. 2024. 2
- [43] Kaipeng Zeng, Bo Yang, Xin Zhao, Yu Zhang, Fan Nie, Xiaokang Yang, Yaohui Jin, and Yanyan Xu. Ualign: pushing the limit of template-free retrosynthesis prediction with unsupervised smiles alignment. *Journal of Cheminformatics*, 16(1):80, 2024. 5, 6
- [44] Di Zhang, Wei Liu, Qian Tan, Jingdan Chen, Hang Yan, Yuliang Yan, Jiatong Li, Weiran Huang, Xiangyu Yue, Wanli Ouyang, et al. Chemllm: A chemical large language model. *arXiv preprint arXiv:2402.06852*, 2024. 1, 2, 5, 6, 7
- [45] Zihan Zhao, Da Ma, Lu Chen, Liangtai Sun, Zihao Li, Yi Xia, Bo Chen, Hongshen Xu, Zichen Zhu, Su Zhu, et al. Chemdfm: a large language foundation model for chemistry. *arXiv preprint arXiv:2401.14818*, 2024. 1, 2, 5
- [46] Shuangjia Zheng, Jiahua Rao, Zhongyue Zhang, Jun Xu, and Yuedong Yang. Predicting retrosynthetic reactions using self-corrected transformer neural networks. *Journal of chemical information and modeling*, 60(1):47–55, 2019. 1
- [47] Weihe Zhong et al. Retrosynthesis prediction using an end-to-end graph generative architecture for molecular graph editing. *Nature Communications*, 14(1):3009, 2023. 5, 6
- [48] Zipeng Zhong, Jie Song, Zunlei Feng, Tiantao Liu, Lingxiang Jia, Shaolun Yao, Min Wu, Tingjun Hou, and Mingli Song. Root-aligned smiles: a tight representation for chemical reaction prediction. *Chemical Science*, 13(31):9023–9034, 2022. 2
- [49] Chunting Zhou, Pengfei Liu, Puxin Xu, Srinivasan Iyer, Jiao Sun, Yuning Mao, Xuezhe Ma, Avia Efrat, Ping Yu, Lili Yu, et al. Lima: Less is more for alignment. *Advances in Neural Information Processing Systems*, 36:55006–55021, 2023. 3
- [50] Yifei Zhou, Andrea Zanette, Jiayi Pan, Sergey Levine, and Aviral Kumar. Archer: Training language model agents via hierarchical multi-turn rl. *arXiv preprint arXiv:2402.19446*, 2024. 3

Retro-Expert: Collaborative Reasoning for Interpretable Retrosynthesis

Supplementary Material

This supplemental document provides details on our **Retro-Expert**. In Section 6, we describe the technical implementation of Retro-Expert. Section 7 reports the performance of LLM-based baselines with and without the decision space, along with the prompts used for each baseline. In Section 8, we provide the details of our web lab experiments. Section 9 presents additional ablation studies, including the mitigation of reward hacking and the impact of varying N candidates on prediction performance. In Section 10, we visualize representative reasoning examples to analyze the reasoning capabilities of Retro-Expert, including successful selection and generation cases, as well as failure cases. Section 11 details the interpretability evaluation setup, covering the prompts corresponding to the evaluation metrics, and human evaluation procedures. Finally, Section 12, we provide the prompts applied for all models when evaluated on the out-of-distribution (OOD) dataset.

6. Details of KGPO Module

This section elaborates on the technical implementation details of our Retro-Expert. As depicted in Figure 5, we illustrate the optimization workflow of the KGPO module. This design underscores that the core of our KGPO is to promote critical thinking and reasoning grounded in chemical logic, rather than merely rewarding superficial correctness.

Training Samples. To optimize training efficiency and enhance the model’s ability to learn diverse chemical reaction principles, we did not utilize the entire training dataset directly. Instead, we meticulously curated a high-quality training subset. The original USPTO-50K dataset exhibited a significant long-tailed distribution of reaction templates and severe imbalance in sample quantities across different reaction types.

Our screening strategy was designed to mitigate these data skews. First, consistent with prior work, we employed chemical tools (i.e., RDKit) to extract reaction patterns from the training set using a subgraph pattern matching approach. All samples were partitioned into five tiers based on their template frequency. Subsequently, we performed stratified random sampling: samples were drawn from each frequency-based tier while ensuring that the final selected subset maintained a balanced distribution across reaction types. This process yielded a compact and balanced training set comprising 9k samples, providing a more robust data foundation for the model to learn reliable reasoning capabilities.

For the USPTO-FULL dataset, we applied a similar strategy to obtain a training subset. Due to the absence of

ground-truth reaction type labels, we conducted stratified random sampling solely based on the frequency of extracted reaction patterns, resulting in a final training set of 80k samples.

Training Configuration. We employ reinforcement learning via GPRO (Generalized Reinforcement Learning with Policy Optimization) to optimize the reasoning strategy of the LLM (Qwen2.5-7B-Instruct). To ensure training stability while promoting deep deliberation and exploration, the core hyperparameters are configured as follows: `train_epochs=2`, `max_completion_length=8192`, `temperature=0.7`, `$\beta=0.001$` .

Composite Reward Function. This function is designed to evaluate the complete decision-making process from the reasoning path to the final prediction.

$$r(\mathcal{T}_{\text{LLM}}, y) = \alpha_1 \sum_{i=1}^n r_i + \alpha_2 r_{\text{reactant}} + \alpha_3 r_{\text{format}}, \quad (6)$$

It comprises distinct intermediate rewards (r_1 , r_2 , r_3) corresponding to three sub-tasks: reaction type prediction, reaction center localization, and reactant prediction, respectively. Additionally, r_{reactant} provides the final reward for the correctness of predicted reactants, while r_{format} incentivizes strict adherence to the specified output structure: `<think>...</think><answer>...</answer>`. The corresponding weighting coefficients are set as $\alpha_1 = 1.5$, $\alpha_2 = 1.0$, and $\alpha_3 = 0.2$.

7. Details of Comparison Methods

This section additionally reports the prediction performance of all LLM-based methods under different space settings, along with the prompts used for each method. For chemical LLMs, which inherently adhere to predefined predictive patterns, we strictly follow each model’s evaluation templates to ensure valid predictions. The space-related information was incorporated in accordance with the respective evaluation templates.

For general LLMs, we employ a unified prompt structure identical to that used by our Retro-Expert, instructing the LLM to execute reactant predictions. Crucially, all general LLMs are provided with the identical chemical action space, comprising: (1) predicted reaction types, (2) predicted reaction centers, and (3) Top-4 reactant candidates generated by specialized models.

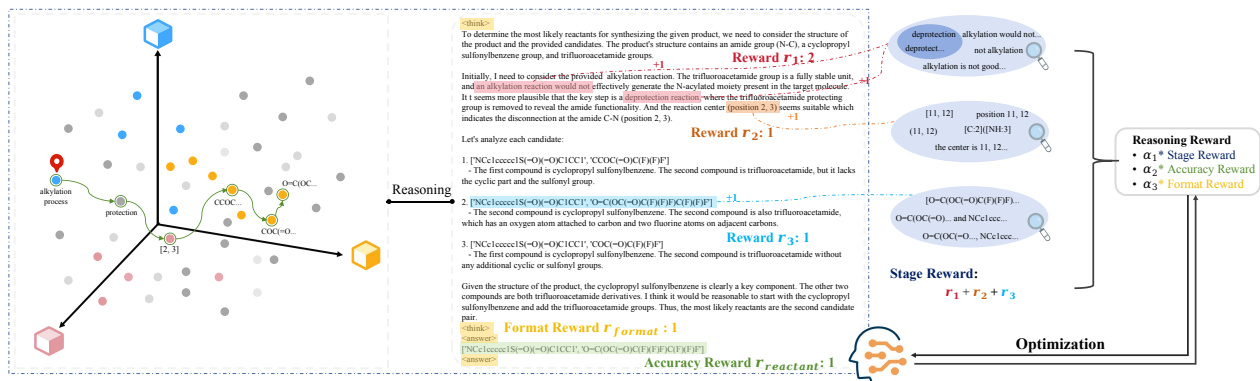


Figure 5. Visualization of the KGPO’s optimization pipeline. Our target is to generate the final answer with an interpretable reasoning pathway by reasoning within the decision space. Thus we further implement a multi-stage reward mechanism that the reasoning text. The mechanism guides the model in two ways: it encourages rejecting incorrect candidates (e.g., “alkylation reaction would not” receives a reward of 1) while promoting inference of the correct reaction type (e.g., “deprotection reaction” receives a reward of 1).

Model	Space Setting	Top-1 Acc (%)	BLEU	Dis↓	Validity↑	MACCS↑	RDK↑	Morgan↑
<i>LLM-based chemical models</i>								
T5Chem	✗	43.64	0.972	8.42	0.982	0.956	0.974	0.925
ChemFormer	✗	27.30	0.769	14.77	0.952	0.782	0.690	0.647
nach0	✗	30.52	0.976	11.91	0.990	0.947	0.977	0.905
ChemLLM	✓	14.60	0.962	16.10	0.981	0.891	0.942	0.805
ChemDFM	✓	12.83	0.869	10.34	0.979	0.851	0.849	0.773
ChemDFM	✗	6.69	0.743	16.62	0.874	0.714	0.807	0.617
ChemDFM	✓	13.64	0.898	11.73	0.841	0.892	0.928	0.819
ChemCrow (+nach0)	✗	30.52	0.976	11.91	0.990	0.947	0.977	0.905
ChemCrow (+nach0)	✓	14.60	0.962	16.10	0.981	0.891	0.942	0.805
<i>LLM-based general models</i>								
InterLM2-Chat-7B	✗	0.73	0.743	19.05	0.706	0.781	0.764	0.589
InterLM2-Chat-7B	✓	24.31	0.957	11.03	0.895	0.945	0.952	0.909
GPT-3.5	✗	1.02	0.836	17.27	0.752	0.788	0.803	0.595
GPT-3.5	✓	32.93	0.969	7.76	0.991	0.952	0.968	0.913
GPT-4o	✗	0.30	0.839	17.68	0.751	0.743	0.646	0.493
GPT-4o	✓	32.85	0.970	7.72	0.990	0.953	0.970	0.914
Gemini-2.5-preview-05-20	✗	4.19	0.790	17.20	0.864	0.765	0.720	0.572
Gemini-2.5-preview-05-20	✓	39.02	0.986	6.63	0.961	0.973	0.989	0.944
Qwen2.5-7B-Instruct	✗	0.02	0.670	30.80	0.668	0.522	0.396	0.289
Qwen2.5-7B-Instruct	✓	37.55	0.971	7.64	0.992	0.961	0.973	0.922
Ours	✓	70.28	0.998	2.27	0.997	0.990	0.996	0.989

Table 9. Comparison with LLM-based models on USPTO-50K. Space Setting indicates whether the model is provided with Top-4 reactant candidates and additional domain knowledge anchors (i.e., reaction types, reaction center) from specialized models. Since T5Chem and ChemFormer process the input by retaining only the product SMILES and directly predicting reactant SMILES, we do not report their performance with space. In contrast, ChemLLM relies on the four candidate reactants for selection and thus only its performance with space is reported.

What are the possible reactants that could have formed the following product?
{Product Standard SMILES}

The prompt for nach0 and ChemCrow.

System:

You are a helpful AI Assistant that provides well-reasoned and detailed responses. You first think about the reasoning process as an internal monologue and then provide the user with the answer. Respond in the following format: `<think>\n...\n</think>\n<answer>\n...\n</answer>`

Assistant:

You are an experienced chemist analyzing chemical retrosynthesis.

Given the standard SMILES representation of the product is: {Product Standard SMILES},

Its automapping version is: {Product Mapped SMILES},

The IUPAC name of the product is: {IUPAC Name}.

The possible reaction type for synthesizing this product is: {Reaction Type}.

The possible reaction center for synthesizing this product is: {Reaction Center}.

Reactants Candidate Set:

- (1) {Top-1 Reactants Candidate}
- (2) {Top-2 Reactants Candidate}
- (3) {Top-3 Reactants Candidate}
- (4) {Top-4 Reactants Candidate}

Please reasonably infer the most likely reactants for synthesizing the product molecule from the Reactants Candidate Set.

Please note that `<answer>\n...\n</answer>` should only contain the reactants.

The prompt for our Retro-Expert training.

There is a single choice question about chemistry. Answer the question by replying A, B, C, or D.

Question: What are the usual materials employed for creating {Product Standard SMILES}? Its automapping version is: {Product Mapped SMILES}. The IUPAC name of the product is: {IUPAC Name}.

- {Top-1 Reactants Candidate}
- {Top-2 Reactants Candidate}
- {Top-3 Reactants Candidate}
- {Top-4 Reactants Candidate}

Answer:

The prompt for ChemLLM.

Chemical reaction equations are typically expressed in the following form: `reactant1.reactant2.reactant3...>>product`.

In this form, each substance (reactant or product) is represented using the SMILES notation.

Now we will provide you with an incomplete chemical reaction equation, where the missing part is represented by "___". The missing part could consist of one or more substances.

Based on the remaining portions of the reaction equation, please infer what the missing part could be.

Note: Please only provide the missing part in your response, without any additional content.

Incomplete equation:

___ >> {Product Standard SMILES}

The prompt for ChemDFM.

You are an experienced chemist analyzing chemical retrosynthesis.

Given the standard SMILES representation of the product is: {Product Standard SMILES},

Its automapping version is: {Product Mapped SMILES},

The IUPAC name of the product is: {IUPAC Name}.

The possible reaction type for synthesizing this product is: {Reaction Type}.

The possible reaction center for synthesizing this product is: {Reaction Center}.

Reactants Candidate Set:

- (1) {Top-1 Reactants Candidate}
- (2) {Top-2 Reactants Candidate}
- (3) {Top-3 Reactants Candidate}
- (4) {Top-4 Reactants Candidate}

Please reasonably infer the most likely reactants for synthesizing the product molecule from the Reactants Candidate Set. Your response must strictly follow the **Output Format**. Do not include any explanation or additional text.

[Output Format]

answer: <the reactant SMILES>

The prompt for general LLM.

8. Details of Web Lab Experiments

To validate Retro-Expert's practical utility in real-world chemical discovery, we experimentally verify two predicted synthetic routes. Sci-Finder serves as the gold standard for determining route novelty.

8.1. Synthesis of 3-(2-ethoxyphenyl)thiophene

Retro-Expert predicts the target molecule could be synthesized via Suzuki-Miyaura coupling between 1-bromo-2-ethoxybenzene and thiophen-3-ylboronic acid. The reaction scheme is visualized in Figure 6. Furthermore, the occurrence of the reaction and the correct structure of the synthesized product are confirmed by both the ^1H NMR and ^{13}C NMR spectra, as shown in Figure 7.

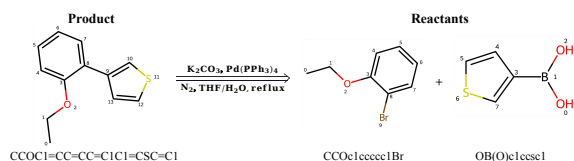


Figure 6. The synthesis path of 3-(2-ethoxyphenyl)thiophene.

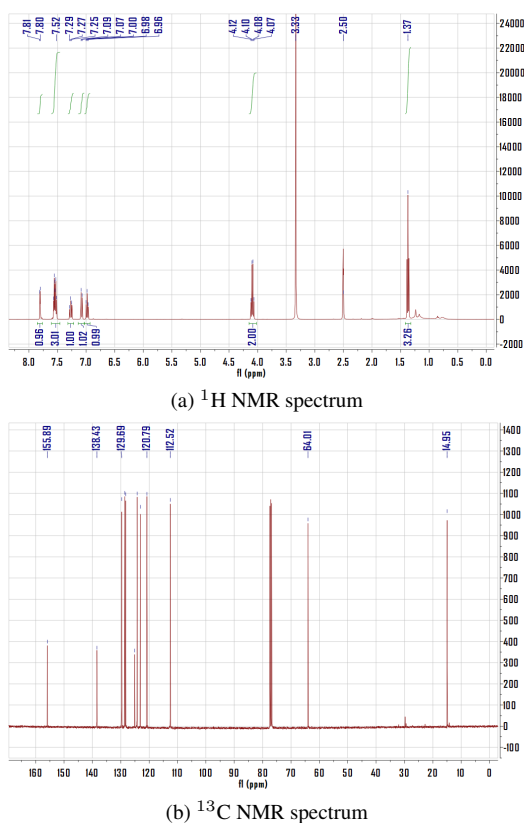


Figure 7. NMR characterization of the synthesized product 3-(2-ethoxyphenyl)thiophene. Both ^1H and ^{13}C NMR spectra support the successful formation and structural integrity of the compound.

The detailed experimental procedure: 1-bromo-2-ethoxybenzene (0.20 g, 1.0 mmol, M1), 3-thiopheneboronic acid (0.15 g, 1.2 mmol, M2), and tetrakis (triphenylphosphine)palladium(0) (0.12 g, 0.1 mmol) were added to a 25 mL three-necked flask. The flask was evacuated and back-

filled with nitrogen three times to ensure an oxygen-free atmosphere. An aqueous solution of K_2CO_3 (1 M) was prepared and set aside. Subsequently, 8 mL of tetrahydrofuran (THF) was added to the flask, followed by the addition of 2 mL prepared K_2CO_3 solution, ensuring the reaction system remained under a continuous nitrogen purge throughout the addition. The reaction mixture was heated to reflux at 92°C under a nitrogen atmosphere. Reaction progress was monitored by thin-layer chromatography (TLC). After 40 hours, the reaction was deemed complete. The excess solvent was removed under reduced pressure using a rotary evaporator. The crude residue was diluted with 50 mL of water and extracted with 50 mL of ethyl acetate. The layers were separated, and the extraction process with ethyl acetate was repeated three times. The combined organic extracts were dried over anhydrous Na_2SO_4 . After filtration, the solvent was removed under reduced pressure to afford the crude product as a dark brown liquid. The crude material was purified directly by column chromatography using petroleum ether as the eluent, yielding the desired product as a pale yellow liquid (0.16 g, 79.3%).

8.2. Synthesis of 1-(4-ethoxyphenyl)ethanone

Retro-Expert identified a novel route via Jones oxidation. The synthesis proceeds from 1-(4-ethoxyphenyl)ethanol under acidic conditions using chromium trioxide. A visual representation of the reaction process is provided in Figure 8. Furthermore, the successful oxidation of the secondary alcohol to the corresponding ketone and the formation of the correct product structure were confirmed by ^1H NMR spectroscopy.

^1H NMR spectrum of the synthesized 1-(4-ethoxyphenyl)ethanone, confirming the successful oxidation of the secondary alcohol to a ketone. The observed chemical shifts are consistent with the expected structure.

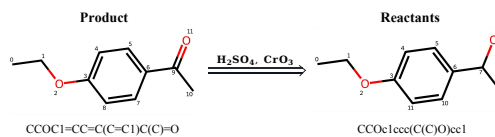


Figure 8. The synthesis path of 1-(4-ethoxyphenyl)ethanone.

The detailed experimental procedure: Chromium trioxide (1.80 g, 0.018 mol) was dissolved in 8.2 mL of deionized water in a 20 mL sample vial. Concentrated sulfuric acid (1.8 mL) was then added dropwise with continuous stirring while maintaining the reaction temperature at 0°C throughout. The resulting orange-red solution constituted the Jones reagent (1.8 M). Separately, 1-(4-ethoxyphenyl)ethanol (0.22 g, 0.013 mol, J1) was dissolved in 10 mL of cold acetone (0°C) in a 25 mL round-bottom flask. While keeping the temperature at 0°C , 2 mL of the freshly prepared Jones reagent was added dropwise.

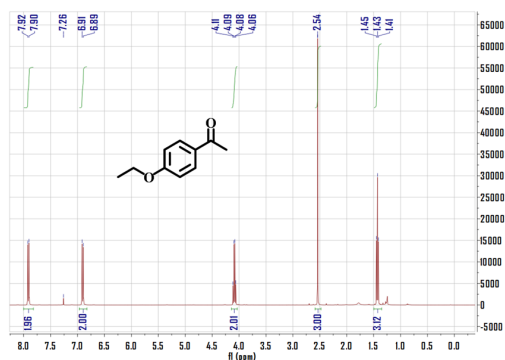


Figure 9. ^1H NMR spectrum of the synthesized 1-(4-ethoxyphenyl)ethanone, confirming the successful oxidation of the secondary alcohol to a ketone. The observed chemical shifts are consistent with the expected structure.

The mixture was stirred at 0°C for 3 hours. Subsequently, 10 mL of ice-cold saturated NaHSO_3 solution was added to quench the reaction, and the pH was adjusted to 13 using ice-cold aqueous KOH . The resulting mixture was extracted with chloroform (3×50 mL) and washed with deionized water. The combined organic layers were dried over anhydrous Na_2SO_4 and concentrated under reduced pressure at room temperature, yielding 125.5 mg of a pale yellow oily product with a yield of 58.82%.

9. Additional Ablation Study

This section presents additional ablation studies.

Reward hacking. Due to the probabilistic bias in the Varying-N candidate results provided by small models, i.e., the correct answer appears in the Top-1 position with significantly higher probability than in other positions. When using result correctness as the reward, the LLM will directly select the first candidate to continuously maximize its reward. To validate the effectiveness of our candidate position shuffling strategy, we visualized the positional distribution of correct answers in the small model’s N candidates and the distribution of positions selected by the LLM. As shown in Figure 10, using the original N candidates from small models results in severe reward hacking, whereas our position shuffling strategy effectively mitigates this issue.

Varying N Candidate. We analyze the impact of using different N values for candidate results during inference on LLM reasoning performance in Table 10. As N increases, the Top-1 reactant prediction accuracy gradually improves. When five or more candidates are provided, the model’s performance stabilizes at 70.8%. This indicates that the model can effectively perform critical reasoning based on the candidate set and generate the optimal answer. To ensure a fair comparison while maintaining competitive performance, we use the Top-4 candidate for reactant-related

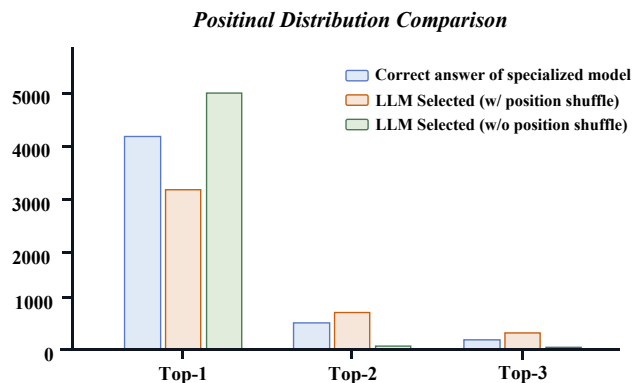


Figure 10. Comparison of positional distributions between the correct answers of small models and the selected positions of LLMs.

N Candidates	1	3	4	5	7
Reactant Top-1	69.9	70.2	70.3	70.8	70.8
Δ	+2.7	+3.0	+3.1	+3.6	+3.6

Table 10. The effect of the N value in small models’ N candidates on large model performance. Δ denotes the improvement relative to the Top-1 accuracy of small models’ reactant prediction (67.2%).

decision space, as chemical LLMs such as ChemLLM rely on four options for selection.

10. Results Analysis

This section showcases visualized examples illustrating Retro-Expert’s reasoning process, highlights both successful and failed cases.

10.1. Successful Reasoning (Selection Scene)

We demonstrate the reasoning processes generated by our Retro-Expert across diverse reaction types (in Figure 11-16). This indicates Retro-Expert’s fundamental competency in executing chemically valid reasoning and making accurate selections within a high-quality chemical action space.

Specifically, our Retro-Expert is capable of performing effective critical reasoning over all candidate options rather than merely selecting the top-1 prediction. During the decision-making process, the model actively incorporates key reaction-related information—such as reaction type and center—to infer plausible mechanisms and eliminate implausible candidates. Notably, Retro-Expert demonstrates strong generalization even for reaction types with limited representation in the training data, and maintains high accuracy across molecules with varying structural complexity. This highlights its ability to perform nuanced, context-aware retrosynthetic reasoning beyond surface-level pattern recognition.

10.2. Successful Reasoning (Generation Scene)

Furthermore, we showcase Retro-Expert's capacity for self-reflection and generation. Crucially, when confronted with suboptimal candidates from all specialized models, Retro-Expert engages in critical analysis and autonomously synthesizes a novel, chemically sound solution (in Figure 17-19).

This generative capability is observed in two distinct yet challenging scenarios. When the candidate set is empty (i.e., no viable options are proposed by the specialized models), Retro-Expert proactively initiates a reasoning process based on available information in the decision space (e.g., reaction type and center). Through this process, it constructs a plausible synthetic route grounded in chemical principles. When all candidate options are present but incorrect, Retro-Expert strategically rejects them and synthesizes an improved solution by critically analyzing the flaws in the proposed candidates and leveraging useful fragments or partial patterns they contain. In both settings, the model demonstrates a high level of autonomy and domain-aware creativity, producing chemically valid outputs even in the absence of reliable reactant candidate.

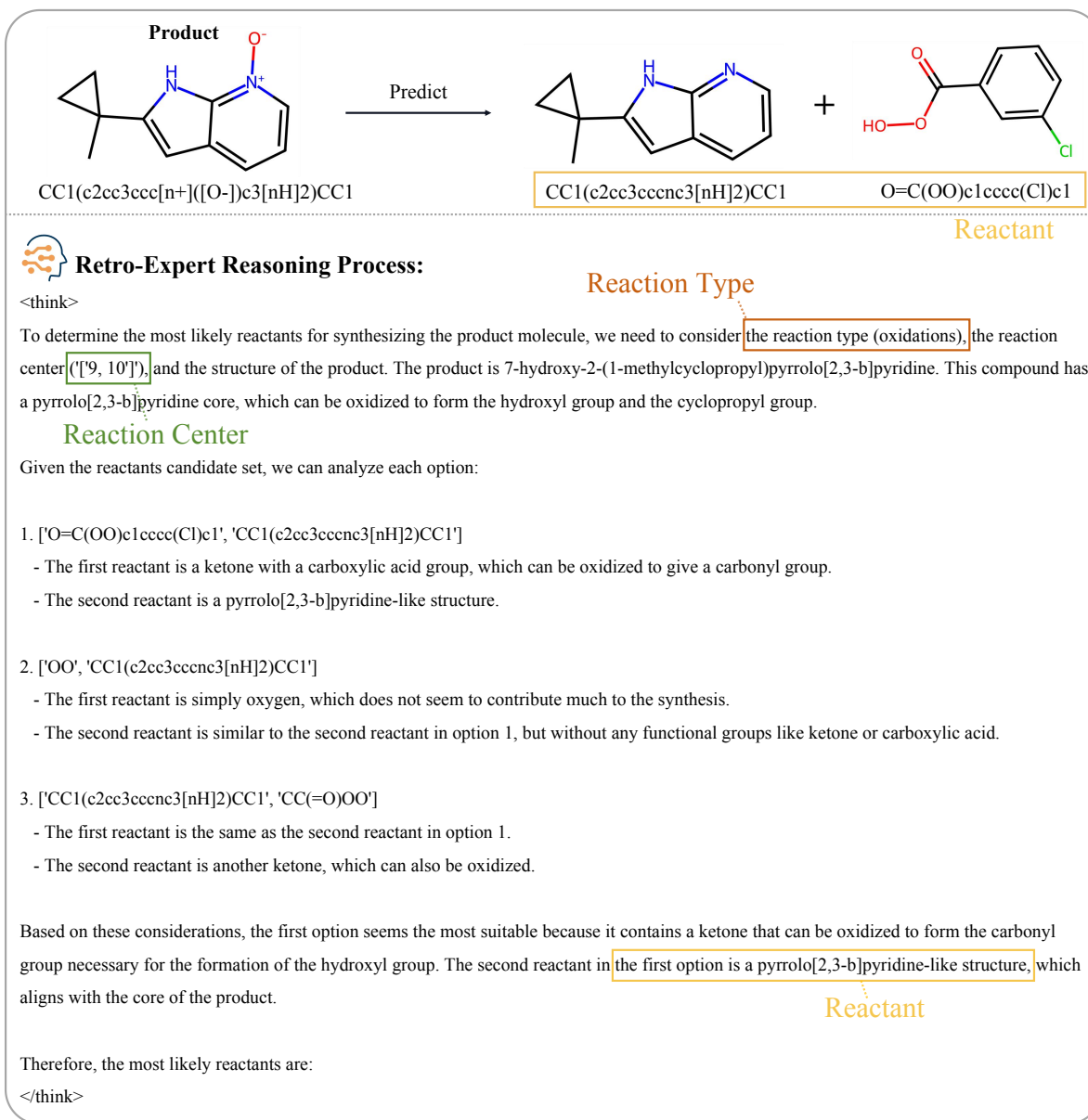


Figure 11. Visualization of reasoning process (1/6) for oxidation reaction.

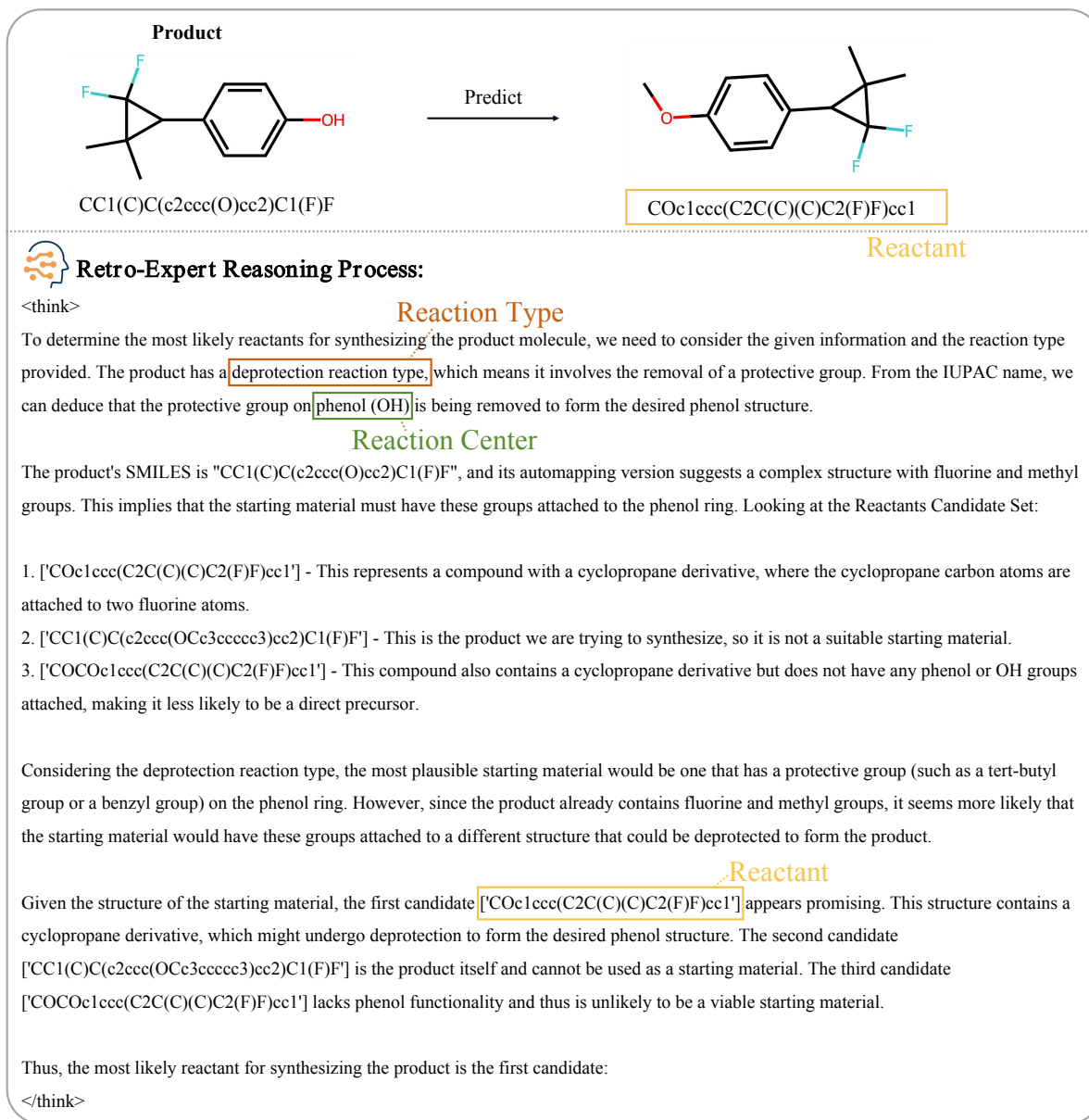


Figure 12. Visualization of reasoning process (2/6) for deprotection reaction.

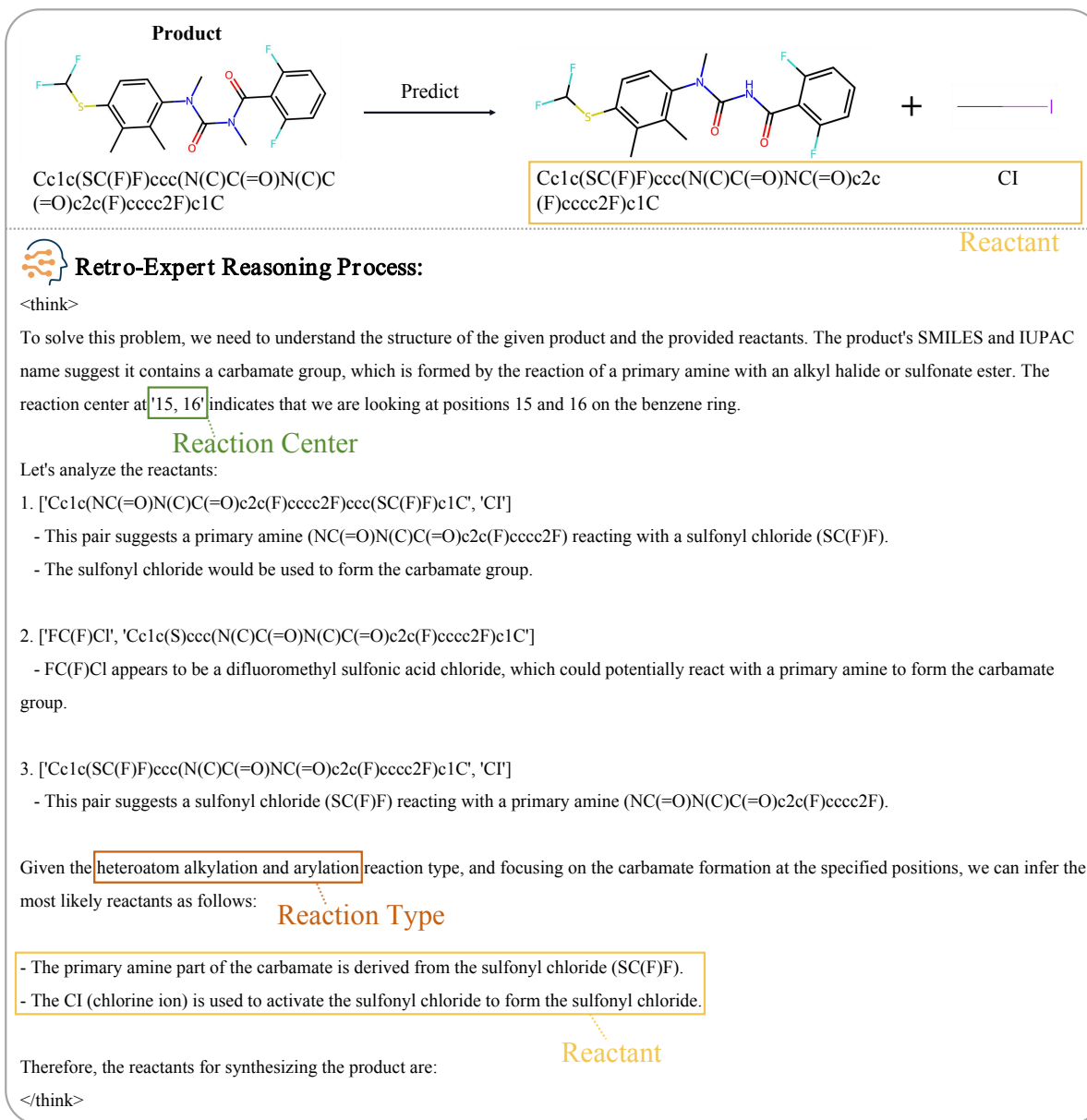


Figure 13. Visualization of reasoning process (3/6) for heteroatom alkylation and arylation reaction.

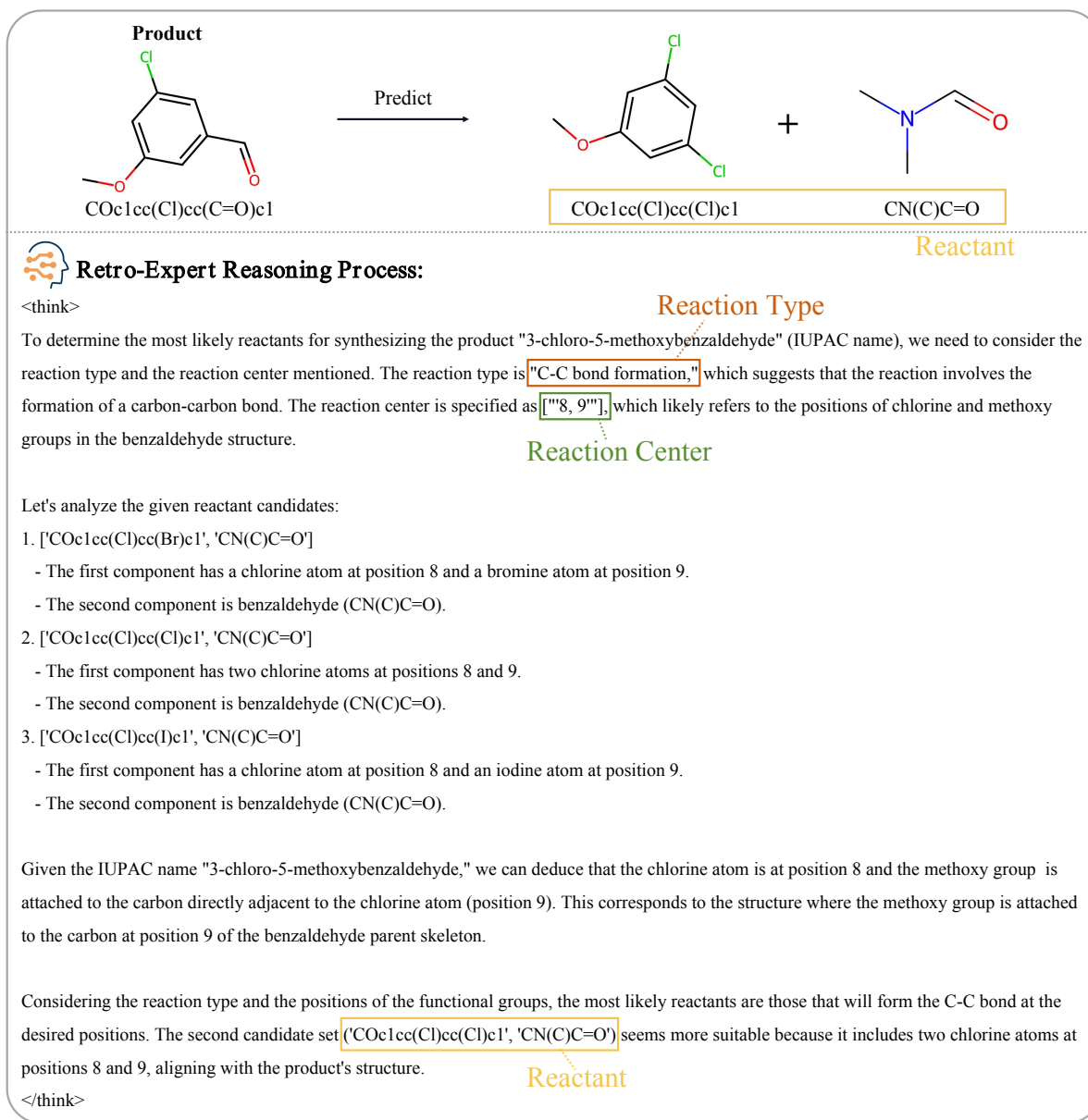


Figure 14. Visualization of reasoning process (4/6) for C-C bond formation reaction.

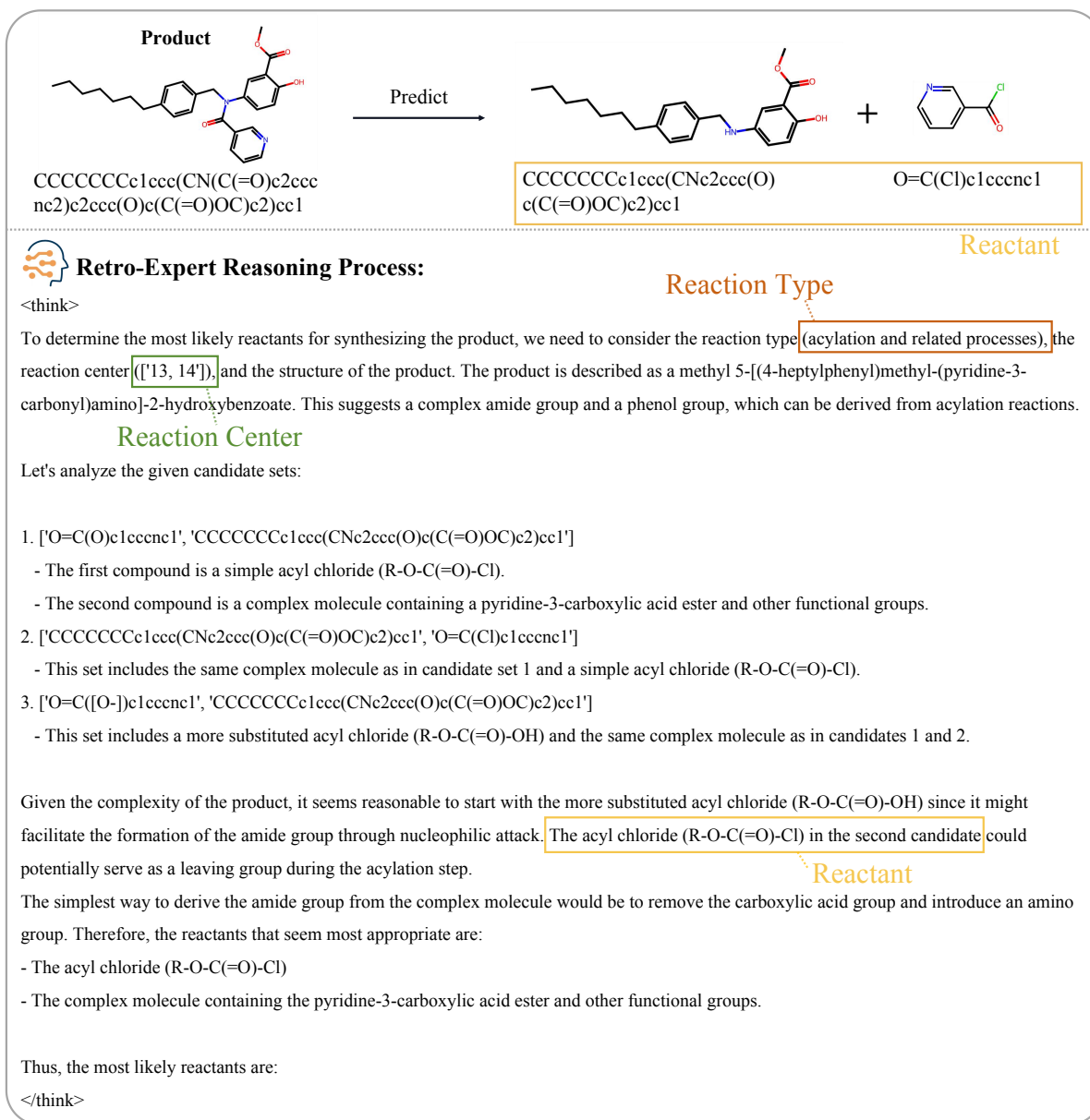


Figure 15. Visualization of reasoning process (5/6) for acylation and related processes reaction.

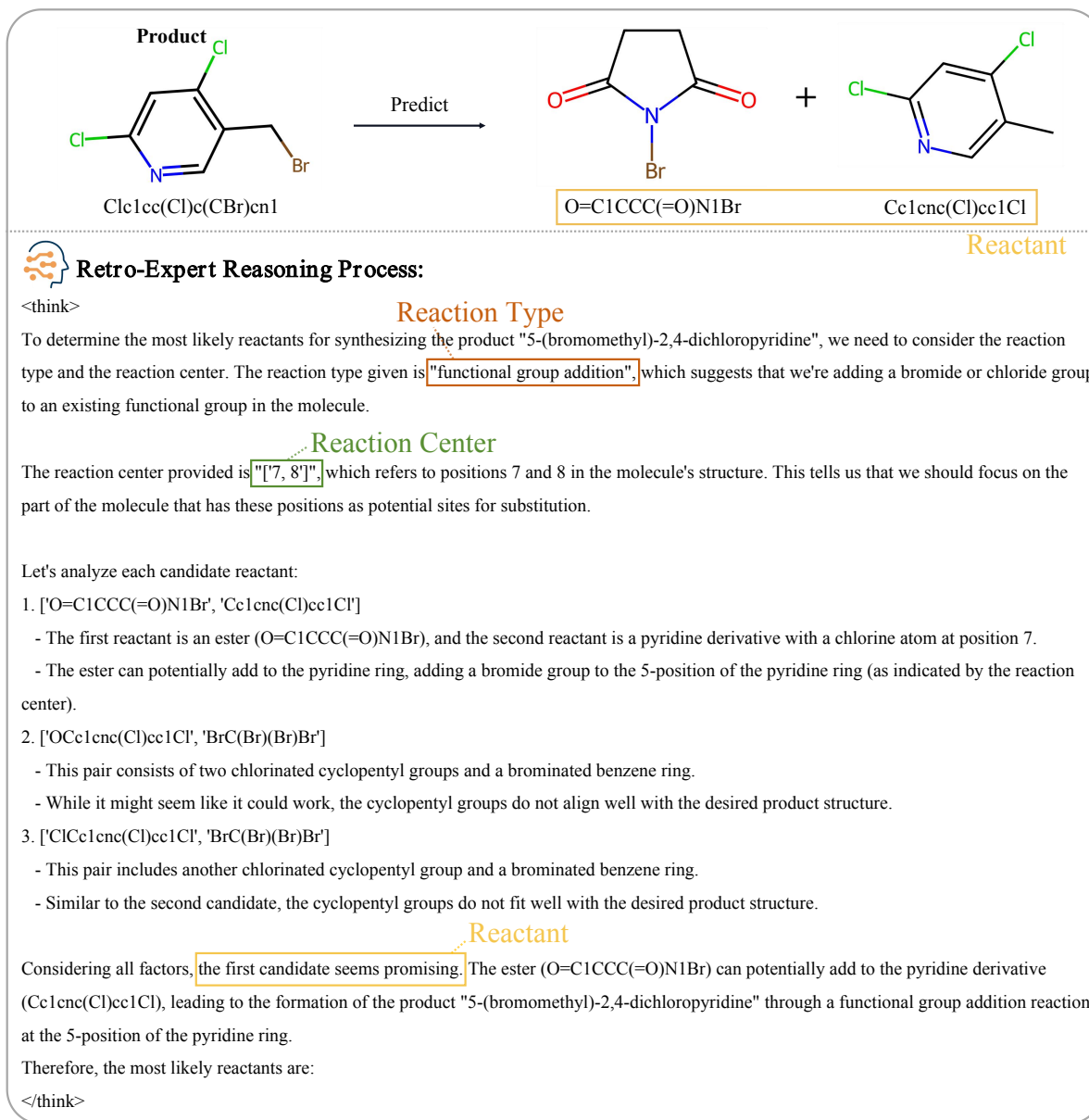


Figure 16. Visualization of reasoning process (6/6) for functional group addition reaction.

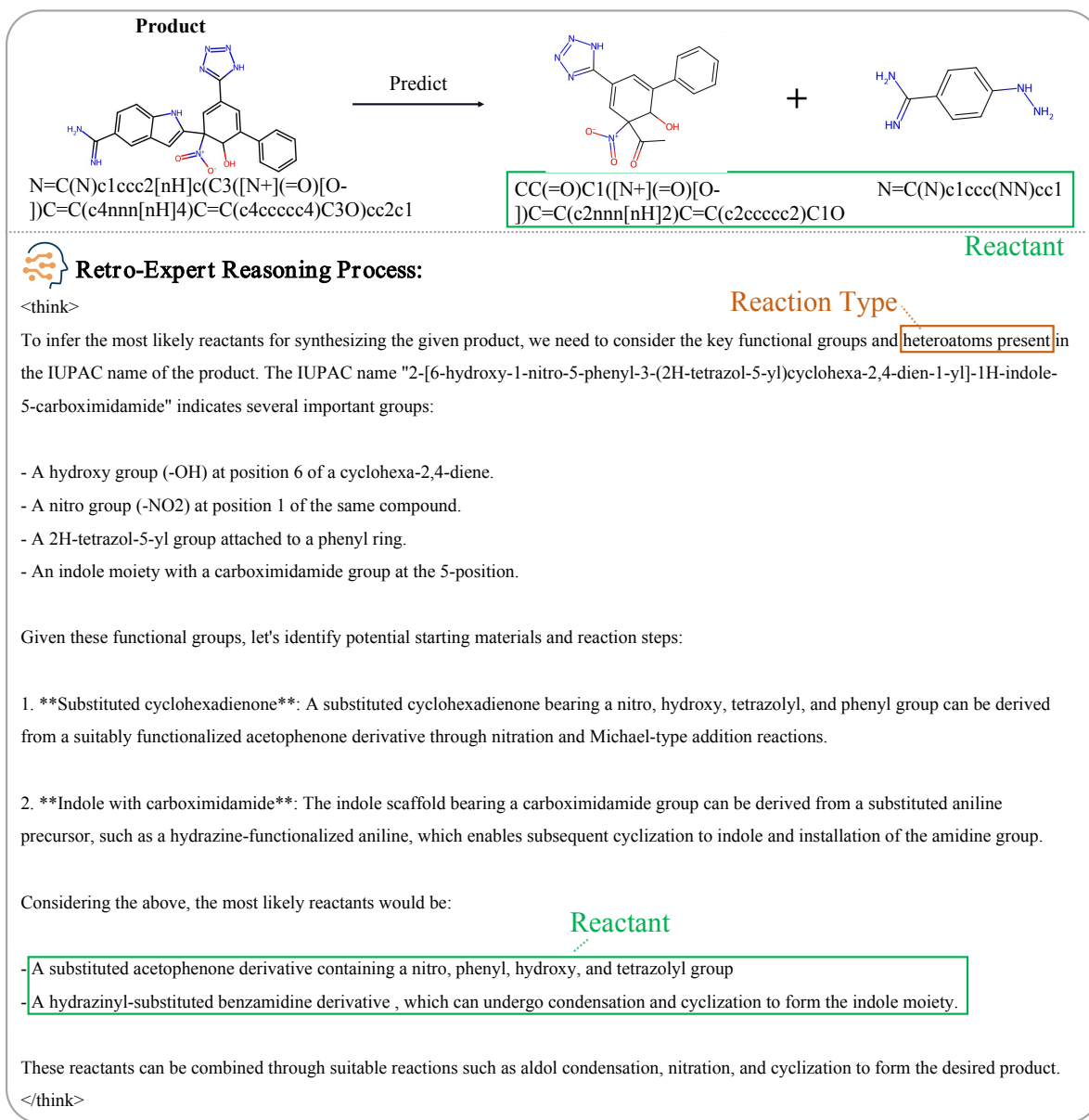


Figure 17. Visualization of the reasoning process (1/3) when no candidate is available.

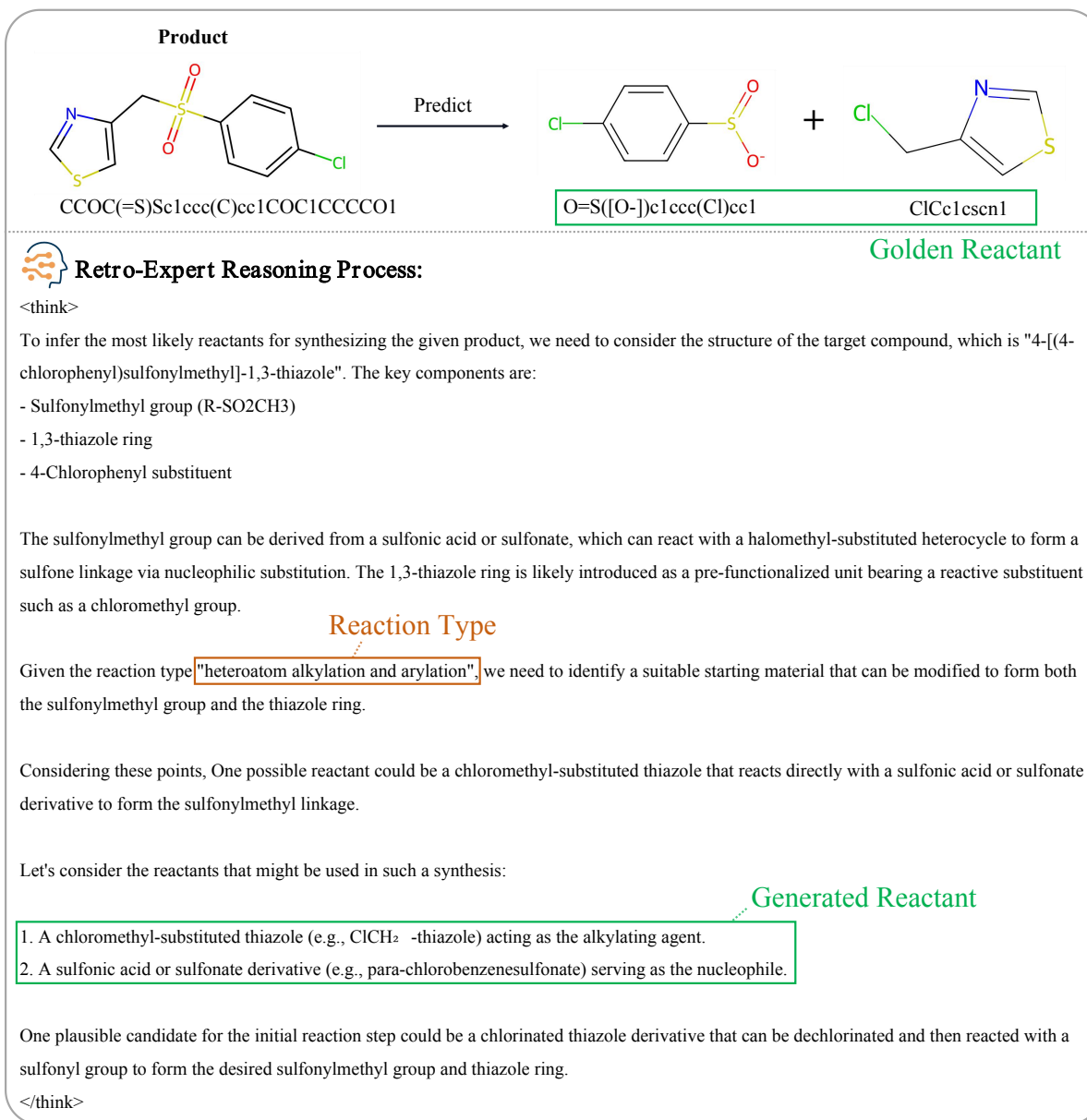


Figure 18. Visualization of the reasoning process (2/3) when no candidate is available.

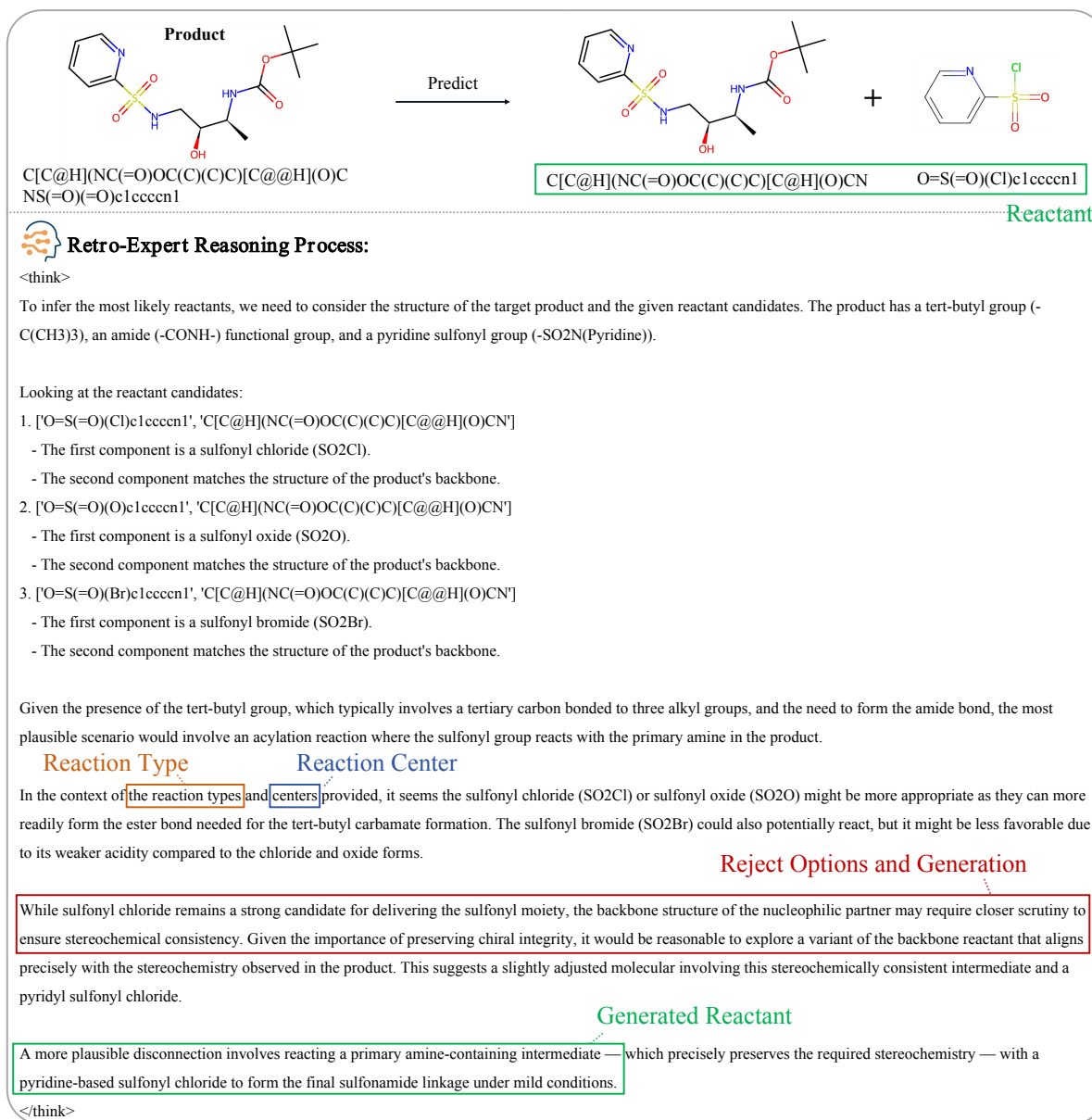


Figure 19. Visualization of the reasoning process (3/3) when the provided candidate is incorrect.

Factual Correctness (FC)

System:

You are an expert in chemical retrosynthetic analysis, responsible for evaluating the quality of reasoning processes generated by retrosynthetic models.

#INSTRUCTIONS:

Based on the following the **Generated Reasoning Process**, conduct a professional assessment across the follow dimensions:

Factual Correctness: Evaluate the presence of factual errors concerning chemical principles within the reasoning description.

[Score 1]: Major factual errors.

[Score 2]: Several errors.

[Score 3]: minor error(s).

[Score 4]: Essentially free of errors.

[Score 5]: Completely accurate.

Evaluations must be grounded in given **Authentic Chemical Synthesis Information** and the results must be strictly formatted according to the specified Output Format.

[Output Format Example]

Factual Correctness:2

.....

Assistant:

Please evaluate the factual correctness of the **Generated Reasoning Process**, based on the given **Authentic Chemical Synthesis Information**.

{Generated Reasoning Process}

Authentic Chemical Synthesis Information:

The product's standard SMILES representation is {Product Standard SMILES}; Its automapping version is {Product Mapped SMILES}; The IUPAC name of the product is {IUPAC Name}.

The reaction type for synthesizing this product is: {The Golden Reaction Type}.

The reaction center of the product molecule is: {The Golden Reaction Center}.

The reactants for synthesizing the product molecule are: {The Golden Reactants}.

Logical Consistency (LC)

System:

You are an expert in chemical retrosynthetic analysis, responsible for evaluating the quality of reasoning processes generated by retrosynthetic models.

#INSTRUCTIONS:

Based on the following the **Generated Reasoning Process**, conduct a professional assessment across the follow dimensions:

Logical Consistency: Determine if conclusions follow logically from premises, analyses, or assumptions without contradictory leaps.

[Score 1]: Conclusion contradicts premises/analysis.

[Score 2]: Partially consistent but with significant logical leaps.

[Score 3]: Partially consistent with only minor leaps.

[Score 4]: Largely fluent and natural.

[Score 5]: Completely fluent and natural.

Evaluations must be grounded in given **Authentic Chemical Synthesis Information** and the results must be strictly formatted according to the specified Output Format.

[Output Format Example]

Logical Consistency:2

.....

Assistant:

Please evaluate the logical consistency of the **Generated Reasoning Process**, based on the given **Authentic Chemical Synthesis Information**.

{Generated Reasoning Process}

Authentic Chemical Synthesis Information:

The product's standard SMILES representation is {Product Standard SMILES}; Its automapping version is {Product Mapped SMILES}; The IUPAC name of the product is {IUPAC Name}.

The reaction type for synthesizing this product is: {The Golden Reaction Type}.

The reaction center of the product molecule is: {The Golden Reaction Center}.

The reactants for synthesizing the product molecule are: {The Golden Reactants}.

The prompt for Factual Correctness (FC).

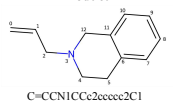
The prompt for Logical Consistency (LC).

11.2. Details of Human Study

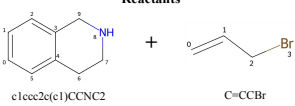
Based on the USPTO-50K test set, we provide the model's interpretable reasoning process along with corresponding ground truth including: reactant-product SMILES, reaction type, and reaction centers. Evaluators were first presented with ground truth information for each sample, then asked to score the interpretable reasoning process. Specifically, they rate the reasoning in terms of (1) Mechanism Accuracy, (2) Factual Correctness, and (3) Logical Consistency. Each criterion is scored on a scale from 1 to 5, with 5 indicating the highest quality. The final score for a sample is calculated as the average of the scores assigned by all evaluators. The evaluation interface layout is shown in Figure 21.

Authentic Chemical Retrosynthesis

Product



Reactants



C=CCN1CC2C=CC=CC2C1 → Predict → c1ccc2c(c1)CCNC2 + C=CCBr

Retro-Expert's Reasoning Process

To determine the most likely reactants for synthesizing the product "1-(3,8-diazabicyclo[3.2.1]octan-8-yl)-2-[4-(tetrazol-1-yl)phenyl]ethanone" (to determine the most likely reactants for synthesizing the product "methyl 4-bromo-3-(cyclopropylmethoxy)benzoate", we need to consider the structure of the product and the given reaction types. The reaction involves heteroatom alkylation and arylation, which typically means adding alkyl groups or substituents to aromatic rings. The product contains a cyclopropyl methoxy group (C(OCC2CC2)c1), a bromine atom (Br), and a methyl group (-CH3).

The product's structure suggests that the starting materials might involve an aromatic ring with a bromine atom and a cyclopropyl methoxy group attached. This would align with the reactants provided:

- [COC(=O)c1ccc(Br)c(O)c1', 'BrCC1CC1'] - This pair involves a brominated benzene ring (COC(=O)c1ccc(Br)c(O)c1) and a cyclopropane derivative (BrCC1CC1).
- [COC(=O)c1ccc(Br)c(O)c1', 'OCC1CC1'] - This pair involves a brominated benzene ring (COC(=O)c1ccc(Br)c(O)c1) and another cyclopropane derivative (OCC1CC1).
- [COC(=O)c1ccc(Br)c(O)c1', 'ClCC1CC1'] - This pair involves a brominated benzene ring (COC(=O)c1ccc(Br)c(O)c1) and a chlorinated cyclopropane derivative (ClCC1CC1).

Considering the reaction type and the structure of the product, the first pair seems more likely because it directly provides a brominated benzene ring and a cyclopropane derivative, which can be further modified to form the desired product.

Wrong Prediction: [COC(=O)c1ccc(Br)c(O)c1', 'BrCC1CC1']
Ground Truth Prediction: [COC(=O)c1ccc(Br)c(O)c1', 'OCC1CC1']

Score

Mechanism Accuracy: 1 2 3 4 5
Factual Correctness: 1 2 3 4 5
Logical Consistency: 1 2 3 4 5

Figure 21. Generated reasoning process rating for human evaluation — assessing the mechanism accuracy, factual correctness, logical consistency of the generated reasoning process on a scale of 1 to 5, with higher scores indicating superior reasoning quality.

12. Details of Out-of-Distribution Analysis

In this section, we provide the identical prompt to all benchmarked models under a uniformly chemical decision space.

There is a single choice question about chemistry. Answer the question by replying A, B, C, or D. The options are TopK predictions.

Question: What are the usual materials employed for creating: {Product Standard SMILES}? Please reasonably infer the most likely reactants for synthesizing the product molecule from the Reactants Candidate Set.

Reactants Candidate Set:

- A. {Option A information in Chembench}
- B. {Option B information in Chembench}
- C. {Option C information in Chembench}
- D. {Option D information in Chembench}

Your response must strictly follow the Output Format. Do not include any explanation or additional text.

[Output Format Example]:

answer: B

The prompt for Out-of-Distribution Analysis.